



**UNIVERSIDAD DE INVESTIGACIÓN DE  
TECNOLOGÍA EXPERIMENTAL YACHAY**

**Escuela de Ciencias Químicas e Ingeniería**

**TÍTULO:**

**Cosmeceuticals products based on Cocoa Pod  
nanocellulose and Bioactive compounds with potential  
UV blocking activity**

Trabajo de integración curricular presentado como requisito para la  
obtención de título de Química

**Autor:**

Andrea María Cevallos  
Guanopatín

**Tutores:**

Lola María De Lima Eljuri,  
MSc.  
Manuel Caetano Sousa,  
Ph.D.

Urcuquí, Octubre 2021

**SECRETARÍA GENERAL**  
**(Vicerrectorado Académico/Cancillería)**  
**ESCUELA DE CIENCIAS QUÍMICAS E INGENIERÍA**  
**CARRERA DE QUÍMICA**  
**ACTA DE DEFENSA No. UITEY-CHE-2022-00002-AD**

A los 7 días del mes de enero de 2022, a las 15:00 horas, de manera virtual mediante videoconferencia, y ante el Tribunal Calificador, integrado por los docentes:

<b>Presidente Tribunal de Defensa</b>	Ph.D. ORDOÑEZ VIVANCO, PAOLA ELIZABETH
<b>Miembro No Tutor</b>	Dra. RODRIGUEZ CABRERA, HORTENSIA MARIA , Ph.D.
<b>Tutor</b>	Mgs. DE LIMA ELJURI, LOLA MARIA

El(la) señor(ita) estudiante **CEVALLOS GUANOPATIN, ANDREA MARIA**, con cédula de identidad No. **0928349448**, de la **ESCUELA DE CIENCIAS QUÍMICAS E INGENIERÍA**, de la Carrera de **QUÍMICA**, aprobada por el Consejo de Educación Superior (CES), mediante Resolución **RPC-SO-39-No.456-2014**, realiza a través de videoconferencia, la sustentación de su trabajo de titulación denominado: **Cosmeceuticals products based on Cocoa Pod nanocellulose and Bioactive compounds with potential UV blocking activity**, previa a la obtención del título de **QUÍMICO/A**.

El citado trabajo de titulación, fue debidamente aprobado por el(los) docente(s):

<b>Tutor</b>	Mgs. DE LIMA ELJURI, LOLA MARIA
--------------	---------------------------------

Y recibió las observaciones de los otros miembros del Tribunal Calificador, las mismas que han sido incorporadas por el(la) estudiante.

Previamente cumplidos los requisitos legales y reglamentarios, el trabajo de titulación fue sustentado por el(la) estudiante y examinado por los miembros del Tribunal Calificador. Escuchada la sustentación del trabajo de titulación a través de videoconferencia, que integró la exposición de el(la) estudiante sobre el contenido de la misma y las preguntas formuladas por los miembros del Tribunal, se califica la sustentación del trabajo de titulación con las siguientes calificaciones:

Tipo	Docente	Calificación
Presidente Tribunal De Defensa	Ph.D. ORDOÑEZ VIVANCO, PAOLA ELIZABETH	10,0
Tutor	Mgs. DE LIMA ELJURI, LOLA MARIA	10,0
Miembro Tribunal De Defensa	Dra. RODRIGUEZ CABRERA, HORTENSIA MARIA , Ph.D.	10,0

Lo que da un promedio de: **10 (Diez punto Cero)**, sobre 10 (diez), equivalente a: **APROBADO**

Para constancia de lo actuado, firman los miembros del Tribunal Calificador, el/la estudiante y el/la secretario ad-hoc.

Certifico que *en cumplimiento del Decreto Ejecutivo 1017 de 16 de marzo de 2020, la defensa de trabajo de titulación (o examen de grado modalidad teórico práctica) se realizó vía virtual, por lo que las firmas de los miembros del Tribunal de Defensa de Grado, constan en forma digital.*

**CEVALLOS GUANOPATIN, ANDREA MARIA**  
**Estudiante**



Firmado electrónicamente por:  
**ANDREA MARIA**  
**CEVALLOS**  
**GUANOPATIN**

**Ph.D. ORDOÑEZ VIVANCO, PAOLA ELIZABETH**  
**Presidente Tribunal de Defensa**

**PAOLA ELIZABETH**  
**ORDONEZ**  
**VIVANCO**  
 Digitally signed by PAOLA ELIZABETH ORDONEZ VIVANCO  
 Date: 2022.01.12 10:05:23 -05'00'

**Mgs. DE LIMA ELJURI, LOLA MARIA**  
**Tutor**

**LOLA**  
**MARIA DE**  
**LIMA ELJURI**  
 Digitally signed by LOLA MARIA DE LIMA ELJURI  
 Date: 2022.01.11 20:22:53 -05'00'

HORTENSIA MARIA  
RODRIGUEZ  
CABRERA

Firmado digitalmente por  
HORTENSIA MARIA  
RODRIGUEZ CABRERA  
Fecha: 2022.01.08 17:30:06  
-05'00'

Dra. RODRIGUEZ CABRERA, HORTENSIA MARIA , Ph.D.  
**Miembro No Tutor**

YEPEZ MERLO, MARIELA SOLEDAD  
**Secretario Ad-hoc**



Firmado electrónicamente por:  
**MARIELA  
SOLEDAD YEPEZ  
MERLO**

## AUTORÍA

Yo, **Andrea María Cevallos Guanopatín**, con cédula de identidad 0928349448, declaro que las ideas, juicios, valoraciones, interpretaciones, consultas bibliográficas, definiciones y conceptualizaciones expuestas en el presente trabajo; así cómo, los procedimientos y herramientas utilizadas en la investigación, son de absoluta responsabilidad de el/la autor (a) del trabajo de integración curricular. Así mismo, me acojo a los reglamentos internos de la Universidad de Investigación de Tecnología Experimental Yachay.

Urcuquí, Octubre 2021

---

Andrea María Cevallos Guanopatín  
CI: 0928349448



## AUTORIZACIÓN DE PUBLICACIÓN

Yo, **Andrea María Cevallos Guanopatín**, con cédula de identidad 0928349448, cedo a la Universidad de Investigación de Tecnología Experimental Yachay, los derechos de publicación de la presente obra, sin que deba haber un reconocimiento económico por este concepto. Declaro además que el texto del presente trabajo de titulación no podrá ser cedido a ninguna empresa editorial para su publicación u otros fines, sin contar previamente con la autorización escrita de la Universidad.

Asimismo, autorizo a la Universidad que realice la digitalización y publicación de este trabajo de integración curricular en el repositorio virtual, de conformidad a lo dispuesto en el Art. 144 de la Ley Orgánica de Educación Superior.

Urcuquí, Octubre 2021.

---

Andrea María Cevallos Guanopatín

CI: 0928349448



# *Dedication*

Dedicated to my lovely and supportive parents, grandmothers, and sister.

Andrea María Cevallos Guanopatín





## *Acknowledgements*

I thank God and my family for being my constant support and company during my academic studies.

To the principal, faculty director, and my dear Professors of the School of Chemical Sciences and Engineering for their unconditional support during my academic formation at Yachay Tech University.

To my classmates who became my friends and family during my University journey.

To The School of Biological Sciences and Engineering that cordially opened its laboratories' doors and allowed me to use the equipment necessary for my investigation. Particularly to my Tesis Directors, Lola De Lima and Manuel Caetano, who helped me finish my experimental work despite difficulties during a global pandemic.

Finally, my thanks go to all the people who have supported me to complete my undergraduate thesis directly or indirectly.

Andrea María Cevallos Guanopatín



## *Resumen*

En el presente trabajo se evalúa el potencial de la Cáscara de mazorca de cacao (CPH) para formar un nuevo producto cosmecéutico. El producto cosmecéutico propuesto está formado por la combinación de un derivado de celulosa como sistema de liberación y extracto etanólico como producto activo. La celulosa se extrajo de la Cáscara de masorca de cacao mediante tratamiento alcalino y blanqueo, y la pureza del producto se determina por la blancura del producto y el análisis FTIR. El derivado de celulosa seleccionado para ser sintetizado fue la carboximetilcelulosa debido a su capacidad para solubilizarse en agua y formar hidrogeles. La carboximetilcelulosa se sintetizó variando todos los diferentes parámetros de reacción, incluida la cantidad de hidróxido de sodio, ácido monocloroacético, temperatura y tiempo de reacción. La obtención del producto final se confirmó mediante análisis FTIR y solubilidad del producto final. Fue necesario un procedimiento de purificación para eliminar los diferentes subproductos formados por las reacciones de carboximetilación. La presencia de fenoles y polifenoles en el extracto etanólico de CPH se determinó mediante ensayos fitoquímicos y la determinación de fenoles totales mediante el ensayo de Folin-Ciocalteu. Se obtuvieron películas de hidrogel para dos de los métodos de síntesis, utilizando ácido cítrico como reticulante y extracto etanólico. La actividad protectora UV de las películas obtenidas se demostró mediante la técnica UV-Vis, la mejor protección se encontró con valores de transmitancia de  $(0.98 \pm 0.39)\%T$  a 290nm,  $(3.59 \pm 1.01) \%T$  a 320 nm y  $(29.71 \pm 1.95)\%T$  a 400 nm.

**Palabras clave:** Industria del cacao, carboximetilación, análisis FTIR, cosmecéuticos, protección UV.



## *Abstract*

In the present work, the potential of Cocoa Pod Husk (CPH) to form a new cosmeceutical product is evaluated. The proposed cosmeceutical product is formed by the combination of a cellulose derivative as a delivery system and ethanolic extract as an active product. The cellulose was extracted from de Cocoa pod Husk by alkali and bleaching treatment, and the purity of this product is determined by the whiteness of the product and FTIR analysis. The cellulose derivative was selected to be synthesized as carboxymethyl cellulose because of its ability to solubilize in water and form hydrogels. The carboxymethyl cellulose was synthesized by varying all the different reaction parameters, including the amount of sodium hydroxide, monochloroacetic acid, temperature, and reaction time. The obtention of the final product was confirmed by FTIR analysis and solubility of the final product. A purification procedure was necessary in order to eliminate the different sub-products formed by the carboxymethylation reactions. The presence of phenols and polyphenols at the ethanolic extract of CPH was determined by phytochemical assays and total phenolics determination by Folin–Ciocalteu assay. Hydrogel films were obtained for two of the syntheses methods, by using citric acid as a crosslinker, and ethanolic extract. The UV protective activity of the obtained films was proved UV-Vis technique, the best protection was found with transmittance values of  $(0.98 \pm 0.39)\%T$  at 290nm,  $(3.59 \pm 1.01)\%T$  at 320 nm, and  $(29.71 \pm 1.95)\%T$  at 400nm.

**Keywords:** Cocoa Industry, carboxymethylation, FTIR analysis, Cosmeceuticals, UV protection.



# Contents

<b>Acknowledgements</b>	<b>ix</b>
<b>Resumen</b>	<b>xi</b>
<b>Abstract</b>	<b>xiii</b>
<b>List of Figures</b>	<b>xix</b>
<b>List of Tables</b>	<b>xxi</b>
<b>1 Introduction</b>	<b>1</b>
1.1 Problem Statement . . . . .	2
1.2 Objectives . . . . .	2
1.2.1 Main Objective . . . . .	2
1.2.2 Specific Objectives . . . . .	2
<b>2 Theoretical Frame Work</b>	<b>5</b>
2.1 Incorporation of Cocoa industry waste materials as suitable Raw materials . . . . .	5
2.1.1 Evaluation of morphological and physicochemical properties of Cocoa Pod Husk cellulose . . . . .	6
2.1.2 Skin protection properties and phenolic content of cocoa pod husk . . . . .	8
2.2 Cellulose fibers properties . . . . .	10
2.3 Skin diseases due to sun exposure in Ecuador . . . . .	12
2.4 Cosmeceuticals . . . . .	13
2.4.1 Why Cosmeceuticals? . . . . .	13
2.4.2 Antioxidants in dermatology . . . . .	15
2.4.3 Delivery systems- vehicles . . . . .	16
2.4.4 Hydrogels as delivery systems . . . . .	17
2.4.5 Biopolymer based hydrogel as delivery system for cosmetic products. . . . .	18
2.5 Methods . . . . .	19



2.5.1	Cellulose extraction . . . . .	19
2.5.2	Carboxymethylation . . . . .	19
2.5.3	Maceration . . . . .	20
2.5.4	Crosslinking method . . . . .	21
<b>3</b>	<b>Experimental</b>	<b>23</b>
3.1	Reactives and Equipments . . . . .	23
3.1.1	Biological material . . . . .	23
3.1.2	Equipment . . . . .	23
3.1.3	Reactives . . . . .	23
3.2	Sample Preparation . . . . .	23
3.3	Cellulose extraction . . . . .	24
3.3.1	Alkali treatment . . . . .	24
3.3.2	Delignification . . . . .	24
3.4	X-ray Diffraction (XRD) . . . . .	24
3.5	Carboxymethylation . . . . .	25
3.5.1	Synthesis 1 . . . . .	25
3.5.2	Synthesis 2 . . . . .	26
3.5.3	Synthesis 3 . . . . .	26
3.6	Purification . . . . .	27
3.7	Infrared spectroscopy (FTIR) . . . . .	28
3.8	UV-vis spectroscopy . . . . .	29
3.9	Phenolic Extraction . . . . .	29
3.10	Phytochemical analysis . . . . .	29
3.10.1	Phenolic compounds . . . . .	29
3.10.2	Flavonoids . . . . .	29
3.10.3	Tannins . . . . .	30
3.11	Total phenolic content . . . . .	30
<b>4</b>	<b>Results, Interpretation ,and Discussion</b>	<b>33</b>
4.1	Cellulose extraction . . . . .	33
4.1.1	Alkaline treatment . . . . .	33
4.1.2	Bleaching treatment . . . . .	34
4.2	Carboxymethylation . . . . .	34
4.2.1	Synthesis 1 . . . . .	36
4.2.2	Synthesis 2 . . . . .	38
4.2.3	Synthesis 3 . . . . .	40
4.3	Purification . . . . .	42
4.4	Phenolic compounds . . . . .	43

4.5 Hydrogel preparation . . . . .	45
<b>5 Conclusions</b>	<b>61</b>
<b>6 Recommendations and Future projections</b>	<b>63</b>
6.1 Recommendations . . . . .	63
6.2 Future projections . . . . .	63
<b>A Errors determination</b>	<b>65</b>
A.1 Random errors in the y-direction . . . . .	65
A.2 Estimated standard error of the determined phenolic concentration .	65
<b>Bibliography</b>	<b>67</b>



# List of Figures

2.1	Schematic representation of molecular mechanism of skin aging. . . .	11
2.2	Cellulose repeating unit. . . . .	12
2.3	Diagram of the redox balance in the skin . . . . .	16
2.4	Carboxymethylation reaction mechanism. . . . .	21
2.5	NaCMC and CA crosslinking reaction. . . . .	22
3.1	Sample preparation and cellulose extraction procedure diagram. . . .	25
3.2	Diagram of carboxymethyl synthesis. . . . .	27
3.3	Purification procedure diagram. . . . .	28
4.1	Purified cellulose . . . . .	36
4.2	X-ray Diffraction pattern of CPH-Cellulose. . . . .	37
4.3	FTIR spectra of extracted CPH cellulose. . . . .	37
4.4	FTIR spectra of NaCMC1. . . . .	38
4.5	FTIR spectra of NaCMC2. . . . .	40
4.6	FTIR spectra of NaCMC3. . . . .	41
4.7	NaCMC water dilution after drying. . . . .	42
4.8	Glycolic acid formation reaction. . . . .	43
4.9	Sodium Sulfate formation reaction. . . . .	43
4.10	Purified NaCMC dilution test. . . . .	45
4.11	FTIR spectra of purified NaCMC1. . . . .	46
4.12	FTIR spectra of purified NaCMC2. . . . .	46
4.13	FTIR spectra of purified NaCMC3. . . . .	47
4.14	Phytochemical test. . . . .	54
4.15	Linear regression of Folin–Ciocalteu (F–C) assay . . . . .	54
4.16	Linearfitlineasconfianza . . . . .	55
4.17	Graph of residuals. . . . .	55
4.18	Transmittance plots of commercial NaCMC films test 1 . . . . .	56
4.19	Transmittance plots of commercial NaCMC films test 2. . . . .	56
4.20	Transmittance plots of CPH-NaCMC films. . . . .	57
4.21	Films prepared with 20% of phenolic extract in solution. . . . .	57
4.22	Hydrogel formed with NaCMC3 and 20% phenolic extract in solution. . . . .	57

4.23 NaCMC3 film FTIR spectra . . . . .	58
4.24 NaCMC2 film FTIR spectra. . . . .	58
4.25 NaCMC3 film without citric acid crosslinker FTIR spectra. . . . .	59

## List of Tables

4.1	FTIR vibrational bands of isolated CPH cellulose. Symbols meaning: w=weak, vw = very weak, sh = shoulder, s=strong, vs = very strong, $\nu$ = stretching, $\delta$ = bending, $\omega$ =wagging, $\rho$ =rocking, as= asymmetric, and s= symmetric, ip= In-plane. . . . .	35
4.2	FTIR vibrational bands of NaCMC1. Symbols meaning: w=weak, vw = very weak, sh = shoulder, s=strong, vs = very strong, $\nu$ = stretching, $\delta$ = bending, as= asymmetric, and s= symmetric. . . . .	39
4.3	FTIR vibrational bands of purified NaCMC1. Symbols meaning: w=weak, vw = very weak, sh = shoulder, s=strong, vs = very strong, $\nu$ = stretching, $\delta$ = bending, as= asymmetric, and s= symmetric. . . . .	44
4.4	Phytochemical test results. . . . .	48
4.5	Phenolic concentration determination by F-C assay . . . . .	48
4.6	Test films with commercial NaCMC at 5% phenolic extract. Transmittance values at UVA and UVB extremes. . . . .	50
4.7	Test films with commercial NaCMC at 10% phenolic extract. Transmittance values at UVA and UVB extremes. . . . .	50
4.8	Test films with commercial NaCMC at 15% phenolic extract. Transmittance values at UVA and UVB extremes. . . . .	50
4.9	Test films with commercial NaCMC at 20% phenolic extract. Transmittance values at UVA and UVB extremes. . . . .	50
4.10	Test films with commercial NaCMC blank. Transmittance values at UVA and UVB extremes. . . . .	51
4.11	CPH-NaCMC2 film with 20 percent of phenolic extract. Transmittance values at UVA and UVB extremes. . . . .	51
4.12	CPH-NaCMC3 films with 20 percent of phenolic extract. Transmittance values at UVA and UVB extremes. . . . .	51
4.13	FTIR vibrational bands of NaCMC3 film. Symbols meaning: w=weak, vw = very weak, sh = shoulder, s=strong, vs = very strong, $\nu$ = stretching, $\delta$ = bending, as= asymmetric, and s= symmetric. . . . .	52

4.14 FTIR vibrational bands of NaCMC3 film without citric acid. Symbols meaning: w=weak, vw = very weak, sh = shoulder, s=strong, vs = very strong, $\nu$ = stretching, $\delta$ = bending, as= asymmetric, and s=symmetric. . . . .	53
A.1 F-C data analysis . . . . .	66
A.2 <i>Average</i> <sub><math>S_{x_0}</math></sub> . . . . .	66

# Chapter 1

## Introduction

Cellulose is a biopolymer that is most widely obtained from vegetable fibers. There is an increased interest in this substance because of its biodegradability and compatibility with most natural polymers [1–3]. The chemical structure of cellulose fibers provides them with a hydrophilic character. Depending on the source of the cellulose extraction and its degree of water affinity, cellulose can produce gel-like morphologies [1, 4]. Cellulose fibers can be isolated from cocoa pod husks (CPH) using alkaline treatment and bleaching processes [5, 6]. CPH is also an alternative to expanding the sources of phenolic substances, showing significantly higher total phenolics and antioxidant activity than cocoa beans [7, 8]. Phenolic compounds found in CPH are associated with antioxidants and anti-wrinkle and UV protective activities [7, 9–11]. Gel-type products can increase the bioavailability of the extracts onto the skin and are easy to apply to the skin surface [12]. Since the influence of phenolic compounds on certain biological functions and the appearance of skin have been associated with long-term effects, and they are intended to be applied topically, they can be considered as cosmeceutical [13]. Cosmeceutical products are related to preventing various dermatologic conditions, like skin cancer, photoaging, and skin rejuvenation during wound healing [14, 15]. The present research describes a procedure to determine the presence of phenolic components extracted by maceration from CPH, obtain the CPH cellulose, examine its purity, and prepare water-soluble carboxymethyl-cellulose derived from it.

This work comprises the established problem statement that gives an idea of the development of research objectives. The background includes all the information about the use of cosmeceutical, the properties related to cosmeceutical products, cellulose properties, delivery of bioactive compounds, hydrogels as a delivery system, phytochemicals at CPH, phytochemicals properties, and methodologies used in cellulose extraction, maceration, and carboxymethyl cellulose preparation. Then experimental part presents materials used, reagents, experimental work, and analysis performed. Next, the results and discussion section show all the results obtained during experimentation, and the discussion is based on the bibliographic research.



Results are present in the corresponding tables and figures. Finally, conclusions based on the obtained results and recommendations are present.

## 1.1 Problem Statement

Ecuador's geographical position and the high altitude of a large part of the territory bring a high level of UV radiation. High exposures to UV radiation are closely related to skin affections, radical species generated on the skin affect its integrity in different levels, including skin cancer promotion[16, 17]. On the other hand, Ecuador generates approximately 700,000 tonnes of cocoa pod husks waste each year; the beans represent only between 21-23% of the total cocoa fruit weight, and the rest is discarded on the ground. This practice yields a series of plant diseases that negatively affect cocoa plantations [6].

In this study, we propose a solution that will mitigate both before mentioned problems through the development of a gel-like material based on the cellulose and phenolic compounds extracted from the cocoa pod husk; therefore, taking advantage of the waste produced by the cocoa industry and offering a product with skin protective properties.

## 1.2 Objectives

### 1.2.1 Main Objective

Development and characterization of cosmeceutical composite hydrogels with potential skin cosmetic applications, based on cocoa pod husks cellulose, blended with a phenolic and polyphenolic extract from the same part of the fruit.

### 1.2.2 Specific Objectives

- Determine suitable conditions for the extraction of cellulose from cocoa pod husk.
- Study the physicochemical properties of the extracted cellulose, crystallinity percentage by X-ray Diffraction, and chemical nature by Infrared spectroscopy.
- Design a proper extraction method for active compounds and a convenient methodology to examine their presence.
- Design an appropriate methodology for the synthesis and purification of sodium carboxymethyl cellulose from purified cellulose.

- Determine optimal conditions for hydrogel preparation and evaluate hydrogel efficacy as a sunscreen agent.



## Chapter 2

# Theoretical Frame Work

### 2.1 Incorporation of Cocoa industry waste materials as suitable Raw materials

Cellulose nanofibers (CNF) can be isolated from cocoa (*Theobroma cacao* L.) pod husks, using the alkaline treatment and ultrasonication to disintegrate micro-sized fibrils, and adding a minimal concentration of sulfuric acid [5, 6]. Cocoa production is an agricultural sector with economic relevance, especially in some countries of Africa, Asia, and Latin America. Cocoa beans are the only part that is generally used for industrial purposes as they represent only 21-23% of the total cocoa fruit, by the other side cocoa pod husk represents 70–75% of the fruit, giving a range of 700 and 750 kg of waste from each ton of fruit produced. The chemical compositions on a dry basis (%w/w); cellulose 35,4%, hemicellulose 37%, lignin 14,7% and remaining are ash, moisture content and others [6]. Since now all of the CPH that are demonstrated to contain some phytochemicals, enzyme, and polysaccharide were usually left in plantations with no proper treatment causing environmental problems like plant diseases as black pod rot [18].

Due to the recent interest in developing products based on bioactive materials caused by the global necessity of using materials obtained from renewable sources, the scientific community has started to work on these innovative products. Cellulose is now on tendency because it is found as an option to produce high-value biocomposite materials with new advanced functionalities, and also because cellulose represents 50% of natural biomass. Due to the high degree of compatibility of cellulose with other polymers, it is a worldwide trend to create green and biocompatible products that take advantage of its availability, biodegradability, and renewable origin [19].

Cellulose nanocrystals (CNC) present a series of good bio-physicochemical characteristics, such as low toxicity, stiffness, lightweight, low thermal expansion, gas

impermeability, thermal stability, hydrophilic absorbent, adaptable surface chemistry, and remarkable mechanical and optical properties, like high tensile strength and elasticity, optical transparency, and anisotropic behavior. In addition, CNCs are capable to self-organize and producing materials with improved appearance, thermal properties, and barrier performances[7, 19]. These properties can be exploited in numerous fields, including the pharmaceutical industry and regenerative medicine, with the development of new formulations and drug delivery systems, such as emulsions, liposomes, aerogels and hydrogels, DNA hybrid nanomaterials, polymeric films, etc[8, 19]. Nanocellulose fibers can be dispersed homogeneously in water without aggregation and sedimentation. The suspension prepared with even 1wt% nanofiber can exhibit a very high viscosity because of the large hydrophilic surface area formed by cellulose fibers and entanglement. The cellulose nanofibers can behave in water like dissolved polymers and maintain a good crystallinity at the same time. Additionally to the unique properties of the suspension formed in water, it is found that hydrogels can be prepared using cellulose nanofibers, soaking it in alkaline aqueous solutions and then neutralizing it [7]. Even with a lot of information in the literature about the obtention of nanofibrils from conventional lignocellulosic materials, the investigation of new sources is always relevant. The cocoa pod husk is seen as an alternative to expand the sources of nanomaterials that can also add important functionalities to the composites like adding flavonoids, antioxidants, and carotenoids and also to improve the barrier and mechanical characteristics to biocomposites demonstrating its great potential on nanocomposites production [8].

### **2.1.1 Evaluation of morphological and physicochemical properties of Cocoa Pod Husk cellulose**

Z. Daud, A. Zawawi, M. Sari, et al.(2013) had made previous analyses of the surface morphology of cocoa pod husks from Malaysia varieties, using Scanning Electron Microscopy (SEM) for the visualization. This analysis was made to understand the distribution and fiber arrangement of the agriculture waste that is significant for its study. This SEM image for cocoa pod husk shows that it has lamella-shaped particles on the surface. It also shows that fiber produces a rough and thick layer of the surface to protect its lignocellulosic content because cocoa pod husk indicates a high lignocellulosic content with linear fibrillar arrangements. This characteristic enhances the strength properties of materials or composites that can be produced through it. The cocoa pod husk surface shows to have waxes and other encrusting substances such as hemicelluloses, lignin, and pectin that form a thick layer that allows protecting the important cellulose content inside. The content of encrusting

substances causes the fiber to have an irregular appearance. Besides, the fibrillar arrangements are linear, and the presence of irregular void spaces between the fibrils enhance the strength properties [20].

D.Jimat, F. Putra, S. Sulaiman, et al.(2019) studied the morphology of raw cocoa pod husk and also the micro fibrillated cellulose extracted from cocoa pod husk (CPH–MFC) by alkali chemical and sonification. The morphology showed by field emission scanning electron microscopy (FESEM) for raw cocoa pod husk was native cellulose fiber structure comprised thick-walled fiber and intact structure and by the contrary the extracted CPH–MFC appeared as long interconnected fibrils that tied to a three-dimensional (3D) network, proving that the lignin and hemicellulose were successfully removed, and the fiber was separated into individual cellulose microfibril. The fibers were in the range of 10-20 nm in diameter and several micrometers in length. The FTIR spectrum of extracted cellulose was made to have a structural analysis that proves some correspondence with CPH–MFC. The absorption peak at  $3333.4^{-1}$  proves the presence of hydroxyl groups stretching. The peaks at  $2891.83$  and  $1367.29^{-1}$  were assigned to stretching and deformation vibrations of the C–H group in the glucose unit. Meanwhile, absorption peaks at  $894.29^{-1}$  justify the  $\beta$ -glycosidic linkage between glucose units. The peak at  $1023.72^{-1}$  was assigned to the C–O– group of secondary alcohols and ethers functions existing in the cellulose chain backbone [21]. The FTIR analysis confirms the elimination of the lignin and hemicellulose from the original sample [6]. Another important thing is that the liquid containing the dissolved lignin separated from cellulose is also rich in phenolic compounds [21].

W. Liu, A. Mohanty, L., et al.(2004) have evaluated the effect of alkali treatment on the structure, morphology, and thermal properties of native cellulosic fibers. They evaluate different alkali concentrations and treatment time to see the effect on the quantity of interfibrillar region removed. The result shows increasing alkali concentration and treatment time, more hemicellulose and lignin were eliminated. The results that they obtain for the increasing percent of alkali solution and time result in a clean fiber surface, and only a small amount of material remained in the interfibrillar region. After the removal of hemicellulose, the interaction between fibers is reduced, which makes the fibers easier to separate. The ESEM images further support the FTIR and XPS results to verify the removal of hemicellulose and lignin. TGA and differential thermal gravimetric analysis (DTGA) show that alkali solution treatment improved the thermal stability shifted the decomposition temperature to a higher temperature. Finally, they conclude that by increasing both parameters concentration of alkali solution and treatment time, the thermal stability of fibers is also increased [22]. The alkaline treatment also disintegrates the cellulose

in small size crystallites by depolymerization of the inherent cellulose structure, so it is necessary to take into account that using strong alkalinity, the cellulose fibrils can have undesirable degradation. The election of the alkali solution concentration must be controlled to only hydrolyze the fiber surface [6].

### **2.1.2 Skin protection properties and phenolic content of cocoa pod husk**

In a previous experiment, cocoa pod aqueous ethanol extract (CPE) was analyzed to determine its toxicity. The cells normally die in the presence of toxic substances, so a cellular cultivates was done to determine the activity of the extract; the result was that cells don't die but been multiply which not only shows that the extract is not toxic but also shows that the CPE promotes cellular renovation. The cell renovation provides skin with new cells, which make the skin appear smooth and supple, which makes CPE a potential anti-wrinkle agent. Also, the half-maximal effective concentration (EC50) was determined and indicated no cytotoxicity affecting up to  $46.88 \mu\text{g/mL}$  of the extract [12].

The composition of cocoa pod husk was determined and reported with total phenolic content at 45.6-46.4 mg gallic acid equivalent of soluble phenolic while 32,3% carbohydrate, 21.44% lignin, 19.2% sugars, 8.6% protein, and 27.7% minerals [23]. Also, a determination of total phenolic content (TPC) was done in order to recognize its level of antioxidant; this was reported at  $49.54 \pm 3.39$  mg gallic acid equivalent (GAE) per gram sample and total flavonoid content (TFC) at  $22.42 + 0.98$  mg rutin equivalent per gram sample [12]. In another investigation, an even higher TPC value was reported at  $56.5 \pm 0.57$  mg GAE/g [24].

The cacao fruit's phenolic content includes many classes of molecules, like, catechins, epicatechins, anthocyanins, proanthocyanidins, phenolic acids, condensed tannins, other flavonoids, and some minor compounds [25]. Besides, it has been reported that pod husk of cocoa contained significantly higher antioxidant activity and total phenolics than cocoa beans [26].

Polyphenols are related to health preservation due to antioxidant activity; they can act as proton donor-scavenging radicals, inhibitors of enzymes that increase oxidative stress, chelate metals, bind carbohydrates and proteins. Polyphenols are divided into four groups based on the number of phenolic rings and of the structural elements; these groups are phenolic acids, lignans, flavonoids, and stilbenes. Flavonoids exhibit higher antioxidant activity than phenolic acids due to the arrangement of multiple hydroxyl groups in their structure[26]. Between the phenolic

compounds reported at cocoa pod extract, it is found that procyanidin, apigenin, ellagic acid, and rosmarinic acid show antioxidant activity that contributes to the improvement of skin condition, specifically for wrinkles giving a functional cosmetic effect to cocoa pod extracts[27].

Abdul Karim et al.(2014) reported the composition of cocoa pod extract (CPE) determined by UHPLC. These investigators also associate the different compounds found in the extract with different activities that have been previously proved by other investigators[28]. The antioxidant activity of cocoa pods was initially related to the presence of different carboxylic acids as citric and malic acid [29], in addition to phenolic acid and other polyphenols [30–32].The mechanism of antioxidant action has long been associated with the ability of antioxidants to deactivate free radicals in the organism. In the case of citric acid, its antioxidant activity has been related to the antiradical properties due to its reaction with hydroxyl radicals [29], while the antioxidant activity of malic acid has been related to the reactions with both molecular oxygen and hydrogen peroxide formed. Additionally, the presence of flavonol compounds, catechin, and quercetin, have the ability to reduce the free radical formation and to scavenge free radicals[33–36]. And significantly, the presence of terpenoid and resveratrol protects skin from lipid oxidation. Plant extracts with this ability can protect the stratum corneum layer from lipid peroxy radicals[37–39].

Second, the anti-wrinkles activity is related to the inhibition of different enzymes. Elastase is an enzyme that degrades the elastic fibers in human skin [10], catechin flavanols and terpenoids are shown to protect the elastin fibrous structure of the skin by inhibiting the activity of elastase [28]. In addition, the presence of the flavanols, Kaempferol, and quercetin, inhibit the matrix degradation by collagenases activity [38, 40]. And the presence of two types of resveratrol regulates transcription factors and nuclear factors related to the production of metalloproteinases enzymes that are responsible for collagen degradation [38]. The presence of various polyphenols at the same time makes cocoa pod extract an effective helper to maintain collagen longevity in the skin layer.

Lastly, some components present in the cocoa pod extract show skin whitening and UV protective potential. Different types of flavonols, flavanols, stilbenoids, and phenolic acids present in the extract are able to inhibit tyrosinase activity; these include quercetin and resveratrol. Tyrosinase regulates the production of melanin that is primarily responsible for the pigmentation of human skin, so inhibition of this enzyme can be translated to skin whitening properties [9]. In addition, the presence of fatty acids also presents a mechanism of the whitening effect that involves a decrease in tyrosinase level by modulating the ubiquitination of tyrosinase [41, 42] including linoleic acid and oleic acid [43], which are present in the cocoa pod



extract. On the other side, the UV protection on the range of UVB (290-315 nm) and UVA (315-400 nm), its due to the ability of plant extracts that contain flavones and pigments to adsorbs UV light before reaching the skin. The list of flavones contains luteolin and methyl acrylate [44, 45].

The phenolic content of the whole cacao fruit includes many classes of molecules, like, catechins, epicatechins, anthocyanins, proanthocyanidins, phenolic acids, condensed tannins, other flavonoids, and some minor compounds [46]. Besides, it has been reported that pod husk of cocoa contained significantly higher antioxidant activity and total phenolics than cocoa beans [70]. Polyphenols are related to health preservation due to antioxidant activity; they can act as proton donor-scavenging radicals, inhibitors of enzymes that increase oxidative stress, chelate metals, bind carbohydrates and proteins [47].

The exposure and absorbance of UV radiation in the skin can generate reactive oxygen species (ROS) that cause oxidative damage to skin cells. Continuous exposure to UV radiation can cause irreparable damage onto the skin surface that are usually called solar scar and can be manifested wrinkle but more dangerously into skin cancer. Sunscreens had the ability to protect skin from the adverse effects of this kind of radiation, including oxidative stress and DNA damage [48]. The solar spectrum comes in the range of 100 nm to 1 mm that is divided into several regions; the ones that affect the skin are ultraviolet B or UVB from 290 nm to 320 nm, and ultraviolet A or UVA from 320 nm to 400 nm [49]. Cocoa pod extract (CPE) shows a sun screening effect with UV-absorbance at 200-400 nm wavelength. CPE has shown better potential as a UVB sunscreen agent for the cosmetic formulation, and because of its moderate absorbance in UVA is recommended in combination with other sunscreen agents with higher UVA [18, 19].

The different phenomena that promote skin aging and the corresponding inhibitory compounds present in cocoa pod husk are summarized in the scheme presented in Fig.(2.1)

## 2.2 Cellulose fibers properties

Cellulose biopolymer is the substance most widely obtained from vegetable fibers. The cellulose obtained directly from nature tends to be organized in fibrils associated with cellulose molecules that can contain ordered and less ordered regions. This natural fiber is extensively used to create cellulose fiber-reinforced polymers that at present are at the forefront of renewable raw materials. The particular interest in developing this kind of material is to take advantage of the biodegradability

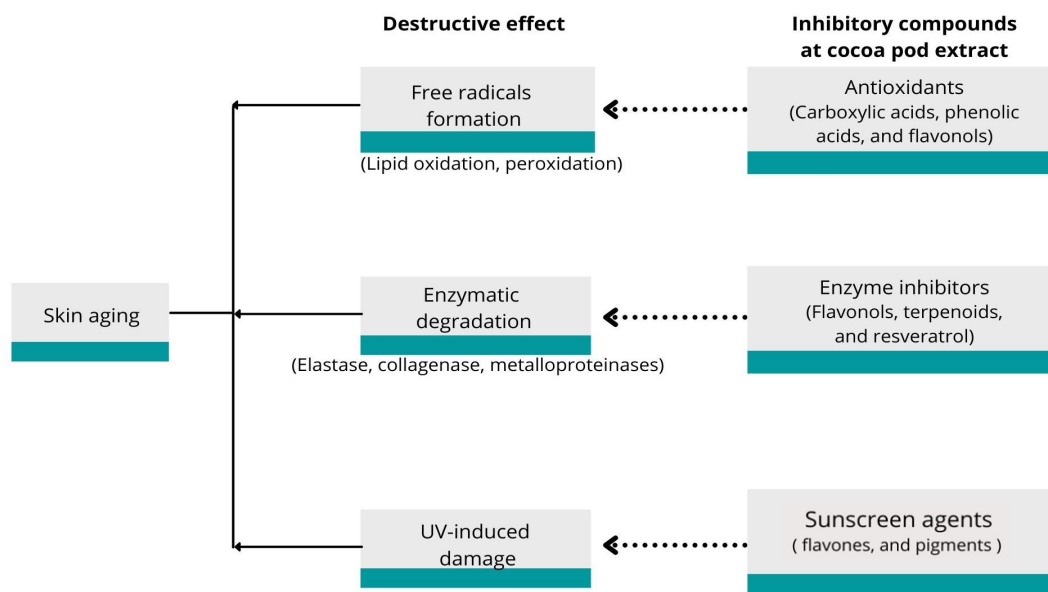


FIGURE 2.1: Schematic representation of molecular mechanism of skin aging.

of cellulose due to it coming from agricultural products. Cellulose fibers are hydrophilic and are very compatible with most natural polymers[1–3].

Cellulose fibers are hydrophilic and are very compatible with most natural polymers, dependent on the source of the cellulose extraction and its degree of water affinity, cellulose with extremely water affinity can produce gel-like morphologies [1]. The hydrophilic character of cellulose comes from its chemical structure Fig. (2.2), this homopolysaccharide consisting of  $\beta$ -D-glucopyranose units linked by glycosidic  $\beta$  (1-4) bonds in a  $4-C_1$  conformation, the ends of the polymer are of different chemical nature one is a ‘normal’  $C_4$ -OH group (non-reducing end), whereas the other  $C_1$ -OH end is in equilibrium with the corresponding aldehyde function (reducing end). Also, this chemical structure is responsible for its high surface energy, biodegradability, and relative thermal fragility. Additionally, the presence of three OH groups in each repeating unit makes this polymer very reactive [4]. Cellulose in nature is found as assemblies of individual cellulose chains forming micro-fibrils; typically, 36 individual cellulose molecules are brought together by a hydrogen bond to create larger units known as elementary fibrils that are highly ordered crystalline regions. These ordered regions are combined with amorphous regions to form larger fibrils. Since nano-sized fillers are predicted to have better mechanical properties is desired to obtain nano cellulose. Nanocellulose can be isolated from the amorphous phase by using an easy performance chemical treatment using acid

hydrolysis, resulting in highly crystalline particles[5].

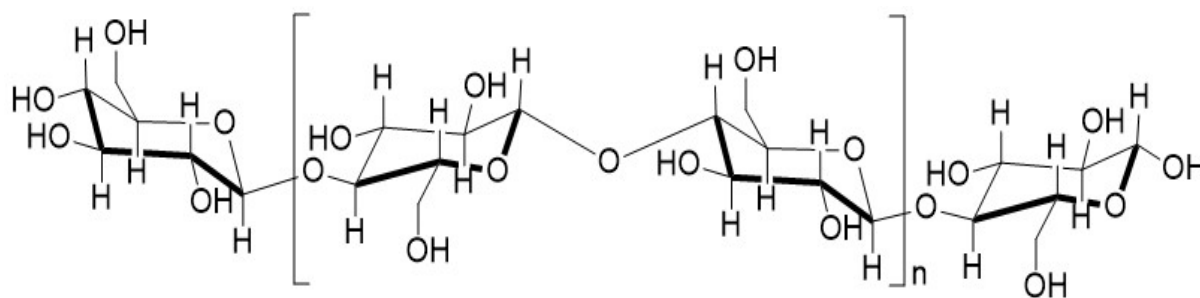


FIGURE 2.2: Cellulose repeating unit.

### 2.3 Skin diseases due to sun exposure in Ecuador

The International Agency for Research on Cancer has registered that in Ecuador in 2020, 441 new cases of melanoma of the skin were reported, and 139 deaths were driven by this condition [50]. Similarly, in 2018 the World Cancer Observatory reported an incidence rate of malignant melanoma of 2.2 per 100,000 population (392 cases), taking 19th place in the list of incidence by cancer site in the country [16]. Second highest prevalent group of neoplasms in Quito, Ecuador are related to sun exposure; these skin lesions can be malignant and premalignant [51]. M. Fors, P. González, C. Viada et al.(2020) also make a study that evaluates the presence of actinic keratoses in agricultural workers, and they found that 35 subjects of the 57 (61.4%) suffer from these premalignant skin lesions, also they mention that these workers do not usually use solar protection[17]. Since Ecuador has an economy that is larger dependent on agriculture, more than 1 million Ecuadorians work directly on the crops, with approximately the middle working on non-perennial crops and the other half on perennial crops [52]. These outdoor occupations with high exposure to ultraviolet (UV) radiation tend to develop nonmelanoma skin cancer [17]. The geographical position of Ecuador makes it most susceptible to the incidence of UV rays because the country is centered in the equator, where the UV radiation is more intense. Another factor that affects the incidence of UV radiation is the height of the territory, and in the case of Ecuador, it is crossed by the Andes Mountains; the intensity of UV radiation increases by 10%–12% per 1000 m of altitude [16]. As to mention before the UV radiation impacts the skin by creating new radical species that are very reactive and induce cancer initiation and promotion. The use of antioxidants for the prevention of this skin affection and especially the use of botanical antioxidants has been recently increasing[53].

## 2.4 Cosmeceuticals

### 2.4.1 Why Cosmeceuticals?

People have developed an increasing interest in their appearance through the years, especially in maintaining a young and healthy aspect of their dermis. We associate cosmetics with only a temporal effect on our appearance that remains while we are using them. On the other hand, pharmaceuticals are drug-like products that affect the structure or function of the human body with a long-term effect [14]. Cosmeceuticals are thought of as physiologically active cosmetics, products that can affect the appearance of skin with a long-term impact. Products in this category are applied topically as cosmetics but contain ingredients that influence the skin's biological functions. The term "cosmeceutical" was introduced in 1984 by dermatologist Dr. Albert Kligman and derived from cosmetics and pharmaceutical words [13]. Even if cosmeceuticals are a current trend in the personal care industry, the term cosmeceutical is not yet recognized by Federal Food, Drug, and Cosmetic Act (FD & C Act), the simply recognizes that a product can be a drug, a cosmetic, or both.

The cosmeceutical industry's exponential growth is driven by the consumers' desire to obtain all the benefits into their skin that the marketing promise to them. This market comprises a variety of products that offer to diminish fine lines and wrinkles, decrease redness, smooth texture, fade discoloration, and give a more youthful appearance to the skin [54]. All of these benefits are obtained without introducing any substance onto the skin or any surgical intervention. In addition, the fact that the majority of these products come from natural sources helps to convince consumers to acquire them. These widely commerce products are exempt from rigid regulation as pharmaceuticals explain their accessible introduction in the global market. Testing these products is normally done by *in vitro* studies usually supported by the cosmetic companies themselves[15].

The lack of a standardization process for evaluating cosmeceutical's effectiveness makes it challenging to determine the efficacy of a certain cosmeceutical in the treatment of a particular skin condition [55]. Since cosmeceuticals are applied by different vehicles, it is necessary to discriminate between the therapeutic effect of the actual active agent and the vehicles themselves. In this way, Dr. Albert Kligman stabilizes a reevaluation that helps determine the effectiveness of a potential cosmeceutical, and this evaluation consists of three important questions [13]. The first question evaluates the capacity of the active ingredient to be effectively delivered in appropriate concentration to the targets in the skin by penetrating the stratum corneum (SC) in a time consistent with its mechanism of action. The second question that relates to the first question is that only an effective active ingredient can

penetrate SC evaluates the existence of a known specific biochemical mechanism of action in the target cell or tissue in human skin for the delivery of the active ingredient. And the last question evaluates if there exists a previous investigation about the active ingredient [56].

In the previous investigations on the utility of cosmeceuticals, it is indicated that the application of cosmeceuticals is principally related to the prevention of various dermatologic conditions, like skin cancer prevention, photoaging, and the rejuvenation of skin during wound healing. Nevertheless, further research about the mechanism of action of the different active principles needs to be done in order to have complete information on their effectiveness. Until today can be mentioned that the most common cosmeceutical agents belong to the following categories: anti-inflammatory agents, depigmenting agents, barrier enhancing agents, antioxidants, and skin renewal agents[14, 15].

The mechanism of action of the most common agents inside this list has been studied, giving information about the level of permeation in the skin barrier and the different effects inside skin cells that make these substances to be recommended for the treatment of specific dermatologic conditions [57]. Salicylic acid is an example of an anti-inflammatory agent. Salicylic acid is a phenolic aromatic acid with both a hydroxyl and carboxyl group attached to the benzene ring, is lipophilic, and easily enters the epidermis and membrane of adnexal structures such as sebaceous glands via hair follicle pores. The lipophilicity of Salicylic acid makes it a good candidate for acne treatment because it can penetrate the pore and subsequent exfoliation of dead skin. In the same group of cosmeceutical agents, there is Glycolic acid that not only has exfoliative properties but also has the ability to activate fibroblasts, promoting cell proliferation and collagen production [15].

After the investigation of the effects of the different cosmeceuticals, it was found a great variety of categories are associated with its action mechanism. Nowadays, some of the categories were reduced to one when a considerable overlap of their actions was found[20]. Finally, the list of cosmeceutical categories was divide into antioxidants, growth factors, peptides, anti-inflammatories/ botanicals, polysaccharides, and pigment-lightening agents, hydroxy acids, retinoid cosmetics, biosensors, muscle relaxants, and dermal fillers, topical enzymes, glycan inhibitors, fatty acids, and plant origin ingredients [58].

Some different categories of cosmeceuticals are subdivided based on the nature of their molecules. Starting with the antioxidants, the distinctive solubility of the molecules that belong to this category makes it relevant to subdivide this category into hydrophobic (lipid-soluble), hydrophilic (water-soluble), and other

antioxidants. Retinoids are classified according to their acidity into acids and non-acids. Also, the ingredients of plant origin are divided into plant extracts, vegetable oils, butter, and vegetable waxes. The different subclassifications are composed of compounds of botanical and non-botanical nature that can come from a variety of sources of which can be easily isolated or can be synthesized entirely or through a precursor [59]. It is necessary to mention that botanical sources are not precisely natural, safe, and healthy, because in the process of extraction, the use of solvents and other reactive for purification can cause contamination, and traces can produce affections into the skin, so the accomplishment of green chemistry needs to be examined [60].

### 2.4.2 Antioxidants in dermatology

Skin, which is the largest organ of the body, is directly exposed to a prooxidative environment, including ultraviolet radiation (UVR) and air pollutants [61]. Both UVA and UVB rays cause damage to the skin, causing sunburn and tanning, and later photoaging with mottled, darkened pigmentation, wrinkles, dryness, leathery texture, and even more severe alterations as precancerous actinic keratoses and actual skin cancer. UVA can interact with ubiquitous environmental pollutants synergistically to initiate skin cancer [62]. Skin acts as a defense barrier against chemical, physical and biological aggressions continuously. Going through different reactions to maintain chemical integrity generates a series of reactive species, including reactive oxygen species (ROS) and other free radicals [61, 63]. These reactive species play pivotal roles in normal cell homeostasis and the cellular responses to various stressors [64], affecting molecules such as proteins, lipids, or DNA [63, 65]. The skin possesses an antioxidant system that deals with oxidative stress to counteract the harmful effects of ROS. Antioxidant enzymes and nonenzymic lessen these changes by intervening at different levels of oxidative processes, like scavenging free radicals and lipid peroxy radicals, by binding metal ions or by removing oxidatively damaged biomolecules [61, 65].

Antioxidants are responsible for directly neutralizing free radicals or chelating metallic ions, which prevents oxidative damage to cells and tissues. The innate antioxidant system of the skin can be quickly depleted in the presence of high levels of radicals where the skin is exposed to high levels of oxidative stress [63, 66]. When the natural antioxidant system is unable to neutralize an excess of radicals, and when there is a decline of the levels of the endogenous antioxidant, it is recommended to supply this antioxidant by the diet (exogenous antioxidants) and also

the application of antioxidant molecules directly on the skin [66]. The topical application of antioxidants enhances sunscreen's action, strengthening skin antioxidative capacity to limit ROS-induced skin damage [61, 67]. Topical antioxidants depending on their nature as hydrophilic, enzymatic or hydrophobic have unique properties and benefits combating free radicals and also reach different parts of the skin cells [68]. Antioxidants have inherent chemical instability so developing an effective multi-sourced topical antioxidant requires creating stable formulations that give effective transcutaneous absorption of the active form, and this is usually challenging [67, 68]. Cosmetics that supply topical antioxidants can combat the effect of pollution onto the skin, improving the structure and function of the skin barrier. Topical antioxidants decrease the oxidation stress and inflammation processes, regulating melanogenesis and removing fibrous protein synthesis in the dermis [69]. A representation of the oxidation and reduction balance in the skin is present in Fig. (2.3)

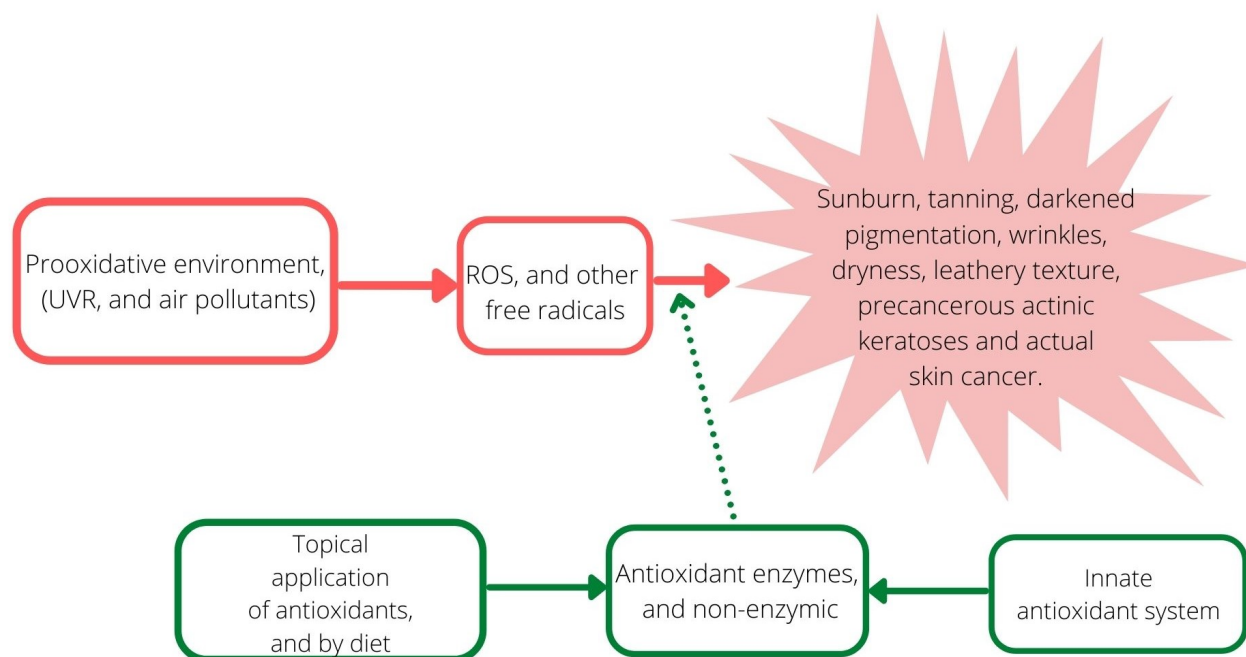


FIGURE 2.3: Diagram of the redox balance in the skin

### 2.4.3 Delivery systems- vehicles

The topical application of active ingredients arms the skin with a reservoir of these different active ingredients, the protection stays on the skin for several days, improving the appearance of the skin in short time periods. The functional agents used in cosmetic products help to by slowing down, stopping, or even reversing environmental and age-related damage that leads to skin wrinkling, discoloration, and loss

of suppleness. For example, the use of antioxidants directly on the skin protects skin against exogenous oxidative stressors occurring during daily life, this is because the active agents target directly the area that needs protection [70]. The topical application effectiveness is dependent on the efficiency of the delivery system to improve the solubility, permeability, and stability of active agents [27, 70]. The vehicle is a mixture of a series of ingredients that forms a three-dimensional matrix, both the ingredients chosen, and manufacturing processes determine the final format of the vehicle the three-dimensional matrix. The vehicle for topical application may carry, transport, or deliver active pharmaceutical ingredient or cosmetic actives. To satisfy the consumer demands the formulated cosmeceutical vehicles should be effective in delivering active compounds through the skin, allowing the active substance to provide the desired effect [27, 71]. It is important to mention that it is difficult to differentiate the effect of vehicles and active substances by separated, however, both are responsible for profoundly modulate the characteristics of the skin and some of its functions [71]. The vehicles not only give a more efficient delivery of active ingredients but also can affect the aesthetics of the product by giving a pleasing application [72].

#### 2.4.4 Hydrogels as delivery systems

Nanohydrogel's properties as a water-swallowable, cross-linked polymeric system that does not dissolve in water, make it a suitable delivery system for cosmeceuticals. The use of nanohydrogels improves the bioavailability and selectivity of the active ingredients. Also, the preparation of hydrogels is simple and can be summarized in two steps, first the polymeric system is synthesized, and then formed biopolymers are cross-linked. The large surface area and hydrophilic nano-sized networks at the three-dimensional structure of the formed nanohydrogels have a direct influence on the bioavailability and stability of active ingredients [25]. Additionally, the soft texture of nanohydrogels provides a comfortable experience for the application, and the ability of a nano hydrogel to encapsulate different active components or drugs with perfect compatibility and efficacy makes its application relevant during skin regeneration [26]. An example of nano delivery systems is based on natural polysaccharides. The tendency of these natural polymers to form hydrogels makes them ideal carriers for oligonucleotides, peptides, proteins, and water-soluble drugs [49]. These delivery systems are generally considered highly safe, stable, biocompatible, and inexpensive biomaterials and can be easily modified and processed according to the required designs and structures for particular applications in different areas [48].



### 2.4.5 Biopolymer based hydrogel as delivery system for cosmetic products.

As mentioned previously, Cellulose nanofibers (CNF) can be isolated from cocoa pod husks by using the alkaline treatment and ultrasonication to disintegrate micro-sized fibrils and adding a minimal concentration of sulfuric acid [5, 6]. Nanofibers with a uniform width can be homogeneously dispersed in water without aggregation and sedimentation and behaved in water like dissolved polymers while maintaining good crystallinity at the same time. The unique properties of nanofiber suspension allow it to prepare hydrogels based on cellulose nanofibers by soaking in alkaline aqueous solutions and then neutralizing them. The hydrogels prepared by this method develop different morphologies and crystalline degrees depending on the concentration of the alkaline solution used for its preparation, presenting different fluidity behavior [7].

Gel-type products can increase the bioavailability of the extracts onto the skin, also are easy to apply onto the skin surface [12]. Hydrogels are characterized because of their biocompatibility, hydrophilicity, pH-responsive behavior, and high porosity that provide them with the capacity of homing fluids and then make a controlled release [73].

Hydrogels made from natural living tissue result in a high-water content that contributes to its biocompatibility, and they also its highly swollen three-dimensional (3D) environment makes it very similar to natural tissues and allows diffusion through the elastic network. Natural hydrogels are achieved through the processing of natural polymer-based materials such as cellulose. Recently, there has been an increase of attention in naturally occurring nanomaterials as cellulose-based materials, especially in the use of cellulose-based hydrogels for tissue engineering. The most important properties for its application are in-vivo swelling properties, mechanical strength, and compatibility with biological tissues facilitating binding. Hydrophilic groups, as, -OH, -COOH, -CONH<sub>2</sub>, and -SO<sub>3</sub>H in polymer chains, are responsible for the swelling properties of hydrogels. High tensile strength, high crystallinity index, and a high degree of polymerization are characteristics of a fine microfibrillar structure [3, 74, 75].

Hydrogels produced with cellulose can be impregnated with active extracts to develop a specific effect on the skin. Due to the benefits shown by the usage of polymer and active extracts blends, these blends found their potential in the cosmeceutical industry as a Bio-mask [76]. Sometimes natural antioxidants present stability issues and difficulties in crossing the transdermal barrier. In this case, the use of delivery systems can be beneficial to protect sensitive active ingredients and also

to enhance the release of these substances onto the skin. Also, employing natural biopolymers as delivery systems is in accordance with the new concerns about the environmental impact [77].

## 2.5 Methods

### 2.5.1 Cellulose extraction

Natural fibers present on plant material are extracted by several processes that increase and decrease the mechanical properties of the objective fiber. The isolation of cellulose from natural sources involves alkali and bleaching treatment of the source material to remove hemicellulose, lignin, pectin, and wax [78, 79]. Hemicellulose affects the properties of cellulose, so it is normally extracted from the raw material. Hemicellulose is very hydrophilic and soluble in alkali solutions. Treatment with high temperature and strong alkali conditions dissolve and also decomposes hemicellulose [78, 80]. Lignin, which is the other major component present in plant structures, has a phenolic nature and is responsible for the structural rigidity of cell walls. Lignin has a hydrophobic character and is also soluble in alkali [78]. In this way, alkali treatment is performed in the raw material before or after bleaching for the semi-chemical degradation of hemicellulose, lignin, and other substances from the external surface of the fiber cell wall [79, 81]. The density of cellulose extracted is increased by the removal of less dense noncellulosic components by the alkaline treatment. After alkali treatment, the resulting material needs to be washed several times with distilled water and neutralized with acetic acid to stop the reaction and remove not reacted hydroxide [81]. On the other side bleaching treatment help to remove the remaining lignin; this treatment can be performed by using a combination of hydrogen peroxide ( $H_2O_2$ ) with sodium hydroxide (NaOH) or sodium chlorite ( $NaClO_2$ ) with acetic acid ( $CH_3COOH$ ). The resulting white fibers show the elimination of residual lignin by oxidation reactions [79].

### 2.5.2 Carboxymethylation

Carboxymethyl cellulose (CMC) is a cellulose derivative, the most consumed cellulose ether. The synthesis of its sodium salt NaCMC is usually performed by etherification reaction of the cellulose hydroxyl group with chloroacetate acid or its salt [11, 82, 83]. During carboxymethylation reaction, cellulose becomes rougher, which results in an increase of the surface area of reaction, giving the chloroacetate group a better chance of reacting with cellulose. The degree of substitution (DS) shows

the efficacy of the introduction of carboxymethyl groups in the place of hydroxyl groups in C6, C2, and C3 positions of cellulose[82, 83]. A water-soluble product requires a DS of a least 0. 4. The DS and solubility are dependent on reaction conditions and had been found that low reaction temperature, decreasing the excess of sodium hydroxide, and increases the time of reaction help to have better results[11]. Reaction variables could enhance the production of sub-products, so the best reaction conditions should be found and carefully controlled. The formation of CMC starts with the obtaining of alkali cellulose by alkaline treatment, where hydroxide ions deprotonate the cellulose hydroxyl groups in C6, C2, and C3 positions, followed by the addition of monochloroacetic acid for the etherification reaction where a second-order nucleophilic substitution happens, between the formed alkoxide ions and the methylene carbon of the monochloroacetic acid[83]. The amounts of reactants sodium chloroacetate, sodium hydroxide, and cellulose must be in the right amount to control the production of sub-products such as sodium glycolate and NaCl, and to produce an optimum degree of substitution. The properties of NaCMC as high viscosity, hydrophilicity, and nontoxicity, make NaCMC suitable for a wide range of applications in the industry as a thickening agent, protective colloid, and film base[11, 83].

### 2.5.3 Maceration

The maceration process consists in place whole or powder plant samples in a stoppered container with the selected combination of solvents, the container is closed to prevent evaporation. The mixture is left to stand for a minimum of 3 days with frequent agitation, after equilibrium is achieved the combined liquids are separated from solids by filtration or decantation [84]. It is necessary to give enough time for the solvent to diffuse to the inside and back to the outside of the cell wall. The extraction of crude drugs is favored by increasing the surface area and mass transfer theory states that the surface area is maximized when particle size is reduced. The solvent is selected depending on the solubility of the objective compounds to be extracted [85]. Phenolics can be extracted from plant material by using different solvents, often in combination with different portions of water. Ethanol and ethanol-water mixtures are recommended because ethanol is not toxic and the polarity can be regulated by using different ethanol/water ratio[86].

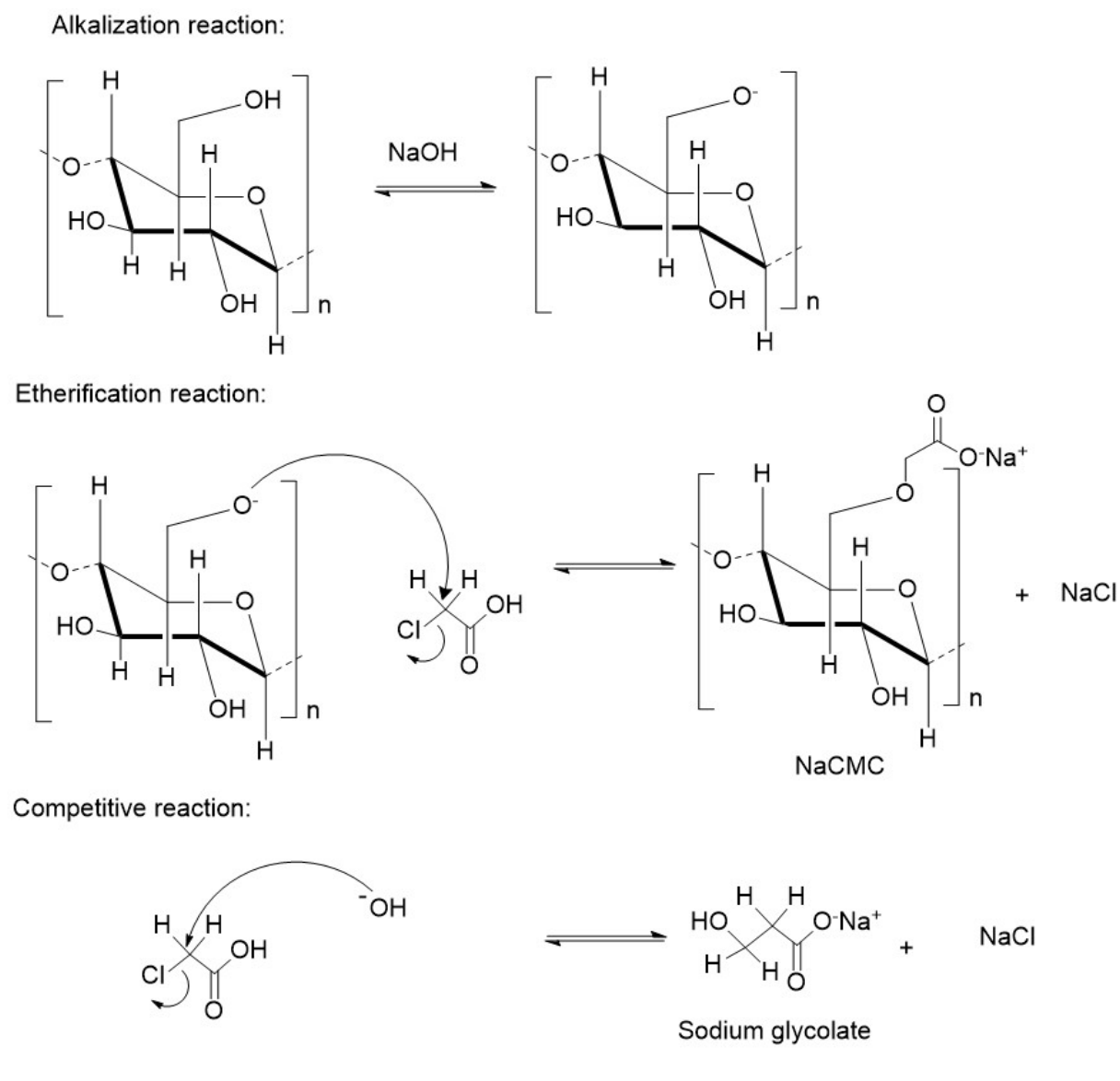


FIGURE 2.4: Carboxymethylation reaction mechanism.

### 2.5.4 Crosslinking method

Cellulose-based hydrogels can be prepared via chemical or physical crosslinking from cellulose aqueous solutions. The list most used cross-linkers in this field include epichlorohydrin, aldehydes, aldehyde-based reagents, urea derivatives, carbodiimides and, multifunctional carboxylic acids [87]. The citric acid (CA) a multifunctional carboxylic acid is an excellent crosslinking agent that is extensively used in industry because it is inexpensive, nontoxic, hydrophilic, additionally, this is a natural organic compound that contains OH groups that allow forming a network in most hydrogel preparation [87, 88]. Citric acid is used as a crosslinking agent in various cellulose derivative systems such as sodium carboxymethyl cellulose (NaCMC). The reaction mechanism is an esterification-crosslinking mechanism[88, 89]. The

mechanism is based on the formation of a cyclic anhydride intermediate by dehydration of citric acid. The cyclic anhydride intermediate reacts with free hydroxyl groups of NaCMC, the carboxylic acid moiety is attached to the cellulose hydroxyl group via esterification, after the reaction, a new carboxylic acid unit in CA is exposed to form a new intramolecular anhydride moiety that can react with hydroxyl groups of another NaCMC chain, and in this way lead to crosslinking [87, 90]. The FTIR spectrum of hydrogel film shows two bands attributed to the carbonyl band, one at approximately  $1742\text{ cm}^{-1}$  that corresponds to the ester carbonyl of the ester formed during crosslinking, and a second band at approximately  $1589\text{ cm}^{-1}$  that corresponds to the carbonyl band of free carboxylic acid groups (carboxylate) [89].

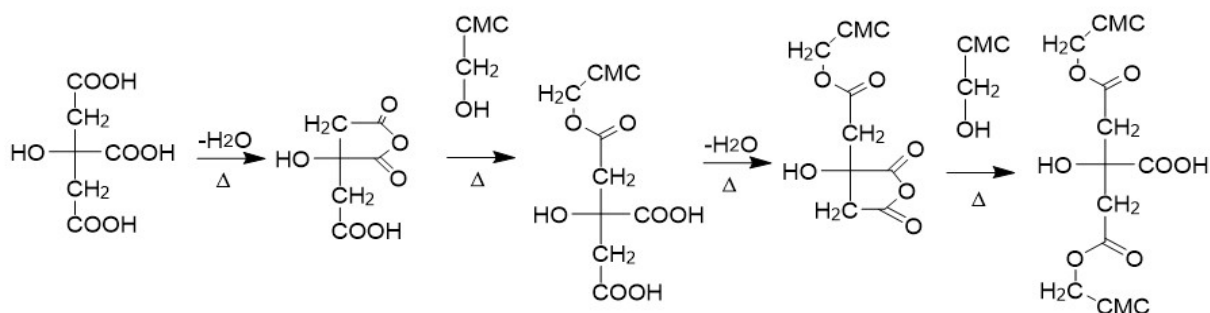


FIGURE 2.5: NaCMC and CA crosslinking reaction.

In the Experimental Chapter, there is a description of the different steps and reactants used in order to develop the different kinds of reactions explained in this chapter. Also, the different mechanisms of evaluation to determine the obtaining of the different intermediaries and final product.

## Chapter 3

# Experimental

### 3.1 Reactives and Equipments

#### 3.1.1 Biological material

Cocoa fruit was obtained from a cocoa Plantation of Quevedo, Los Rios Ecuador.

#### 3.1.2 Equipment

Perkin Elmer UV Lambda 1050, Perkin Elmer UV win lab software, thermometer, Shimadzu, hot and stirrer Plate TOPO, laboratory centrifuge Thermo fisher, SONO-PLUS Bandelin ultrasonic homogenizer, Zuzi spectrophotometer 4211/50, Rotor Mill with 20 Mesh sieve, Flexible Benchtop FTIR Spectrometer Cary 630 FTIR, X-ray diffractometer Mini-flex-600 from Rigaku.

#### 3.1.3 Reactives

Hydrochloric acid Certified ACS PLUS Fisher Chemical (12,1 Normal), Isopropyl Alcohol Certified ACS PLUS Fisher Chemical (99.9%), Glacial Acetic acid (100%) Baker ACS, Methanol HPLC Grade (99.9%) Fisher Chemical, Absolute Ethanol EMSURE Merk, Iron (III) Chloride Hexahydrate (97%), Sodium Nitrite EMSURE Merk (99%), Sodium Hydroxyde, Carboxymethyl cellulose Sodium Salt high viscosity Extra Pure Loba Chemie, Citric acid anhydrous 99.5% Loba Chemie. Chloroacetic acid for synthesis Sigma Aldrich ( $\leq 99.0\%$ ).

### 3.2 Sample Preparation

The cocoa fruits were opened using a knife, and cocoa beans were removed. The cocoa pod husks were oven dry at 40 degrees for one week till complete dryness. Dry cocoa pods were first ground using a grain mill and then ground in a hammer mill

to obtain a smaller particle size; the material obtained was separated into fractions by different sieves mesh. The fractions obtained were 35 mesh, 60 mesh, 120 mesh fraction, 230 mesh, and <230 mesh.

### 3.3 Cellulose extraction

#### 3.3.1 Alkali treatment

The alkali treatment of the starting material is based on previous work of [91, 92], 30 grams of the 60 mesh fraction of CPH were weighed and put into reaction with 600 mL of NaOH 2-5% solution (30g NaOH + 600 mL water), this reaction was done at 80 °C with agitation, the reaction time was complete after 3h obtaining dense and dark wine slurry. After getting cold, the slurry was filtrated by using a strainer with a small mesh size. The obtained material was washed several times with distilled water, using a glass column with a glass fiber filter, and slightly acidified with an acetic acid solution (pH 5).

#### 3.3.2 Delignification

Delignification process was based on [91] work. The obtained material was reacted with a solution containing 975 mL of water, 12mL acetic acid (CH<sub>3</sub>COOH), and 18 g sodium chlorite (NaClO<sub>2</sub>). The reaction was done at 70 °C under the continuous string at 400rpm. After one hour 18 g of chlorite were added to continue the bleaching process. The resulting cellulose was filtered and washed with distilled water using a glass column with a glass fiber filter, centrifuge seven times, and stove dried at 40°C.

### 3.4 X-ray Diffraction (XRD)

The crystalline structure of cellulose was studied by X-ray powder diffraction. A Mini-flex-600 from Rigaku, with a D/tex Ultra 2 detector was used. The X-Ray generator, Ni-filtered Cu K $\alpha$  radiation ( $\lambda = 0.15418$  nm), was fixed at 40 kV, 15 mA. For collecting data, powder samples were placed on sample holder, the selected angular region was  $2\theta = 5^{\circ} - 90^{\circ}$  with a step width of  $0.01^{\circ}$ .

The method used to determine crystallinity index (CI) of cellulose type 1 is the proposed by Segal, the Equation 3.1 is used to calculate the %CI, where  $I_{002}$  corresponds to the height of the peak correspondent to the (002) plane, and  $I_{AM}$  is the lowest height between the peaks correspondent to (002) and (101) planes [93].

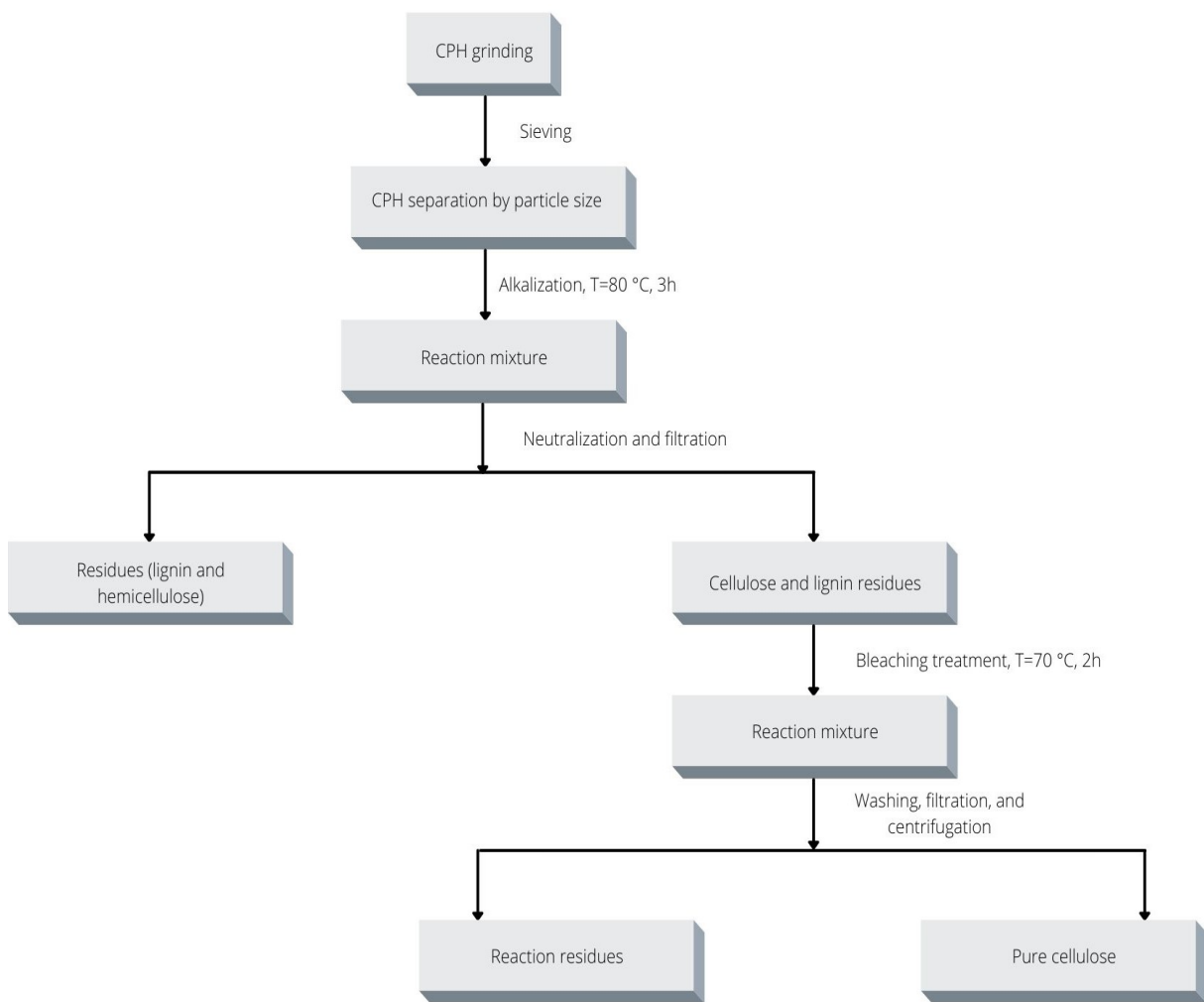


FIGURE 3.1: Sample preparation and cellulose extraction procedure diagram.

$$CI\% = \frac{I_{002} - I_{AM}}{I_{002}} \quad (3.1)$$

## 3.5 Carboxymethylation

### 3.5.1 Synthesis 1

Synthesis 1 is based on [94, 95] works. Carboxymethylation reaction was carried out by first giving an alkali treatment to cellulose. 1g of extracted cellulose was mixed



with 1g of a solution 50% NaOH(w/w%) and sonificated with SONOPULS homogenizer till complete homogenization. After that 20 mL of 50%, NaOH(w/w%) solution was added to the reaction vessel, covered with aluminum foil, and put into agitation 1h at 400 rpm, 35<sup>0</sup>C. For the etherification reaction, 1g of 50%, NaOH(w/w%) solution were premixed with 1.6 g of monochloroacetic acid; the mixture was diluted with 25 mL of pure isopropanol and added to the reaction vessel. The reaction was let 1. 5 h at 75<sup>0</sup>C. After cooling, the reaction was neutralized with concentrate HCl, filtrate and washed with 25 mL of 95% (v/v) ethanol three times. The product was let to oven-dry overnight at 45<sup>0</sup>C.

### 3.5.2 Synthesis 2

Synthesis 2 was based on the [83] work. The carboxymethylation procedure starts with the treatment of 1 g of the obtained cellulose with 2 g of 50%, NaOH(w/w%) solution. The mixture was homogenized by using SONOPULS homogenizer. Once homogenized, the mixture was diluted with 20 g of water. The mixture was let in the reaction under agitation at 35<sup>0</sup>C for 1h. For the second treatment, a total of 2.76 g of chloroacetic acid were premixed with 2 g of 50%, NaOH(w/w%) solution for etherification reaction, this mixture was dissolved in 40 mL 99.9% ethanol and was added to the reaction vessel. The reaction was let 3.5h under agitation at a set temperature of 75<sup>0</sup>C. After cooling, the reaction was filtrated and washed three times with 25 mL 99. 9% ethanol. The product was let to oven-dry overnight at 45<sup>0</sup>C.

### 3.5.3 Synthesis 3

Synthesis 3 is based on [95, 96] works. Carboxymethylcellulose was prepared by dissolving 1g of the obtained cellulose in 100 mL of 85 % ethanol solution, this mixture was homogenized using SONOPULS homogenizer. 4g of NaOH were added to the mixture, covered with aluminum foil, and put into reaction under stirring in a 35<sup>0</sup>C water bath 60 min. 1.6 g monochloroacetic acid was pre-dissolved in 25 mL of ethanol solution and added to the reaction vessel; the temperature was set to 65-70<sup>0</sup>C. After 30 min, 2g of NaOH in 25mL ethanol solution were added, and the reaction was let 1 hour. After the reaction time finished, the reaction vessel was put in a cool water bath let cool. The product was neutralized using concentrate HCl, filtered, and washed three times with 75 % and 95% ethanol solution. The resulting solid was oven-dry overnight at 45<sup>0</sup>C.

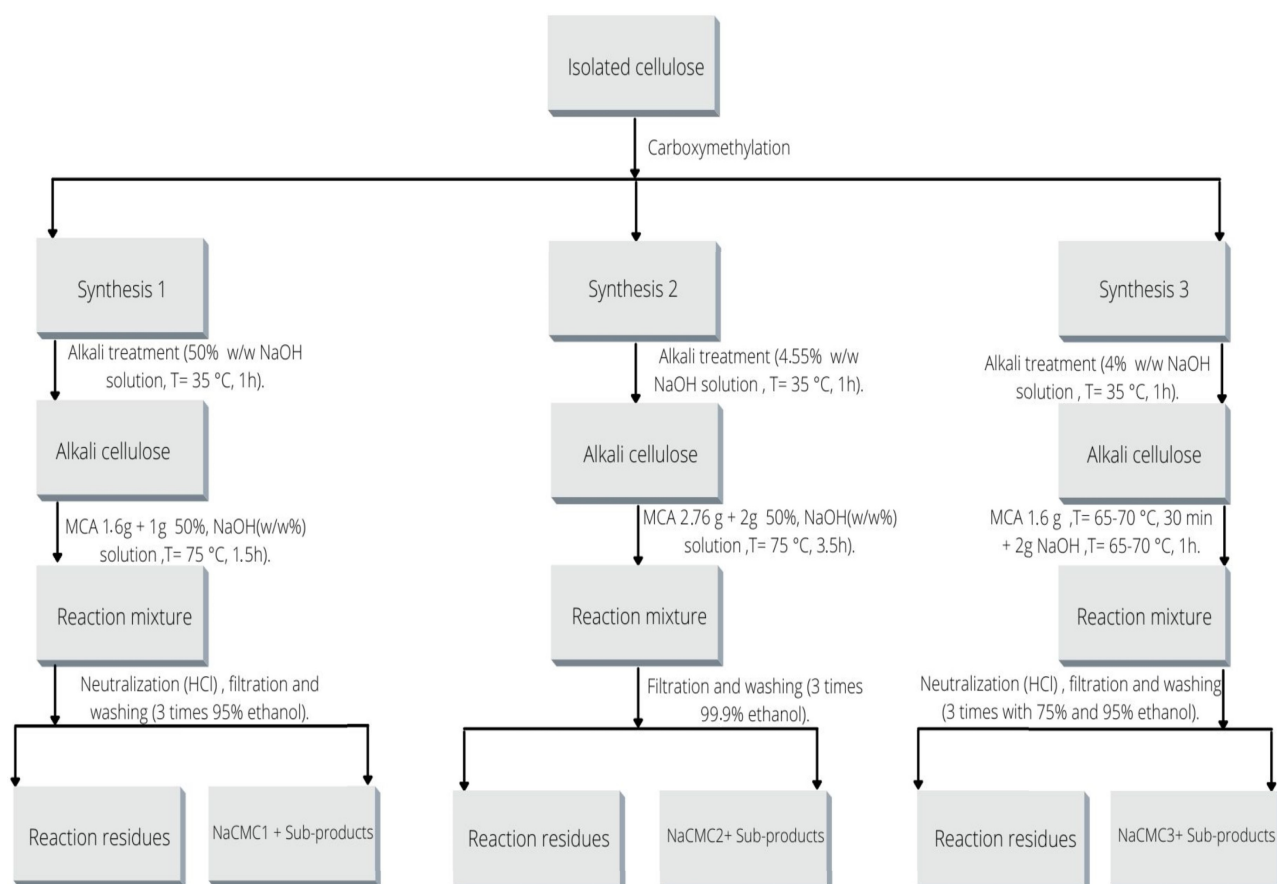


FIGURE 3.2: Diagram of carboxymethyl synthesis with variation of the different variables.

The yield is calculated considering a 1:1 reaction between cellulose and carboxymethyl cellulose:

$$Yield\% = \frac{g_{NaCMC}}{g_{cellulose}} \times 100 \quad (3.2)$$

### 3.6 Purification

The obtained sodium carboxymethylcellulose for the purification step was put in the reaction under magnetically stirring with 100 mL of 20% H<sub>2</sub>SO<sub>4</sub>, at 20-25 °C for 1h. After the reaction was complete the obtained product was filtered and washed with 500 mL of distilled water to eliminate the water-soluble impurities. The product was dry for 1h at 45 °C. After that, the obtained acid form of carboxymethylcellulose was converted again to the sodium salt by reacting with a 4% NaOH in ethanol solution (w/v %) 1.5 h at room temperature. The final product was filtered and washed with

pure ethanol until neutralization and washed two times with pure methanol and one time with isopropanol. The purification procedure is based on [97] work.

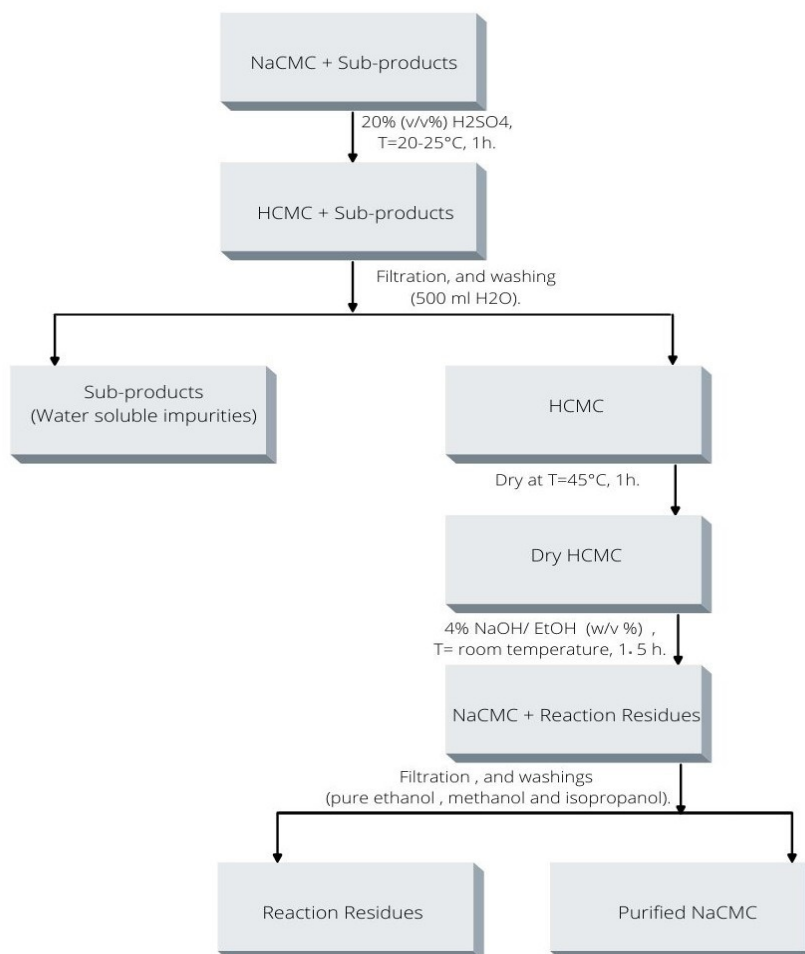


FIGURE 3.3: Purification procedure diagram.

### 3.7 Infrared spectroscopy (FTIR)

All FTIR spectra were performed for the dry samples in the region of 400-4000  $cm^{-1}$  by using Flexible Benchtop FTIR Spectrometer Cary 630 FTIR, the data was analyzed by using OMNIC software.

## 3.8 UV-vis spectroscopy

All transmittance profiles of solid films were conducted on PerkinElmer Lambda 1050 UV-vis spectrophotometer in order to find its UV protective activity. The absorbance measurements were conducted in Zuzi spectrophotometer 4211/50 using 1 cm matched glass cells in order to find the phenolic concentration.

## 3.9 Phenolic Extraction

1g of CPH (0.5 mm particle size) were weighed in an Erlenmeyer flask; in addition, 20 mL of 80% ethanol were added for maceration. The flask was closed with parafilm and covered with aluminum foil, then let in the dark at approximately 48h for maceration. The extract was filtered using a glass filter and refrigerated for posterior use [28].

## 3.10 Phytochemical analysis

### 3.10.1 Phenolic compounds

Ferric Chloride test: 1mL of ethanolic extract was added to a test tube, then 1mL of 2% FeCl<sub>3</sub> solution was added. The presence of a dark color with some blue indicates the presence of phenols [98–101].

Ellagic acid: In a test tube 1mL of the extract was added, then 5 drops of 5% (w/v) glacial acetic acid and 5 drops of 5%(w/v) NaNO<sub>2</sub> were added. After 20 minutes, the presence of a brown precipitate indicates the presence of phenols [102].

### 3.10.2 Flavonoids

Alkaline test: In a test tube with 1mL of the extract, 1mL of 10% NaOH solution was added. A yellow color indicates the presence of flavonoids, and an orange color indicates the presence of flavanones [102].

Shinoda test: A small quantity of magnesium powder was added to a test tube, then 1mL of the ethanolic extract and 5 drops of concentrate HCl were added to the test tube. The colors pink, scarlet, crimson red, or blue indicate flavonoids' presence [100, 103].

### 3.10.3 Tannins

Ferric chloride test: 1mL of ethanolic extract was added to a test tube, then 1mL of water was added, and agitated. 5 drops of 2% FeCl<sub>3</sub> were added. A green precipitate indicates the presence of tannins[98, 101].

## 3.11 Total phenolic content

The procedure to find the Total phenolic concentration is based on [104, 105]works. The calibration curve was done by using gallic acid as a reference, different concentrations of gallic acid were obtained by diluting a stock solution with a concentration of 2 mg/mL. For the Folin–Ciocalteu (F–C) assay, 300  $\mu$ L of each concentration of gallic acid was put into a test tube and 2500  $\mu$ L of 10% F–C reagent was added and the tubes were let in the dark 8 minutes before the next step. Next, 2000  $\mu$ L of 7.5% Na<sub>2</sub>CO<sub>3</sub> were added, the tubes were agitated and let in dark conditions for 2h. After 2h, the absorbance of the samples was measure in a spectrophotometer that was set to a wavelength of 765 nm. The calibration curve was obtained. For the CPH ethanolic extract, three different dilutions were prepared, 1:10, 1:20 ,and 1:40. The same procedure that was used with citric acid for the Folin–Ciocalteu (F–C) assay was followed for each sample. The absorbances were measured and the average phenolic concentration was obtained by using the calibration curve.

Equations used to determine the estimated standard error of the obtained phenolic concentration:

$$S_{y/x} = \sqrt{\frac{\sum_i (y_i - \hat{y}_i)^2}{n - 2}} \quad (3.3)$$

Equation 3.3 represents random errors in the y-direction, the term  $(y_i - \hat{y}_i)$  are the residuals (difference between points calculated by regression line and measured y values), and n is the number of points using in the determination.

$$S_{x_0} = \frac{S_{y/x}}{b} \sqrt{1 + \frac{1}{n} + \frac{(y_0 - \bar{y})^2}{b^2 \sum_i (x_i - \bar{x})^2}} \quad (3.4)$$

Equation 3.4 represents the estimated standard error of the determined phenolic concentration, b represents the slope,  $y_0$  is the measured absorbance of the examined samples,  $\bar{y}$  and  $\bar{x}$  represents the centroid of the regression line (average values), and  $x_i$  the different concentration values at the F-C experiment.

$$Average_{S_{x_0}} = \sqrt{\frac{\sum_i S_{x_0}^2}{n-1}} \quad (3.5)$$

Equation 3.5 represents the estimated standard error of the average phenolic concentration.

The next chapter presents the results of the experimental part and discusses the antecedents of these results in base of bibliographic information. Comparison and interpretation of the results obtained by changing different experimental variables are made on the basis of the different experiences at the experimental work, a visual characteristic of the products, and previously reported works at the bibliography.



## Chapter 4

# Results, Interpretation ,and Discussion

For this work, the Cocoa pod husk (CPH) was obtained directly from a plantation in Quevedo-Los Rios- Ecuador. The initial weight of the CPH just after rupture was 5.13 kg. The weight after complete drying of CPH was 0.77 Kg which indicates a weight loss of 84.99%, which represents the water percentage of the fresh pod husk. The dry CPH was ground and separated into different fractions depending on the grain size, obtaining particles with 35, 60, 120, 230, and < 230 mesh size. The fractions obtained were 68.55 g of the 35 mesh fraction, 107.19 of the 60 mesh fraction, 107.3 g of the 120 mesh fraction, 77.12g of the 230 mesh fraction, and 22.79 g of the <230 mesh.

### 4.1 Cellulose extraction

#### 4.1.1 Alkaline treatment

CPH was treated at high temperature and high pH conditions to remove hemicellulose, lignin, pectin, and wax. During this treatment, the CPH changed from a light brown color firm solid particles to a dense slurry with a dark wine color. Two factors can explain this texture and color change. First, the high values of lignin present in the raw material are susceptible to a color change at different pH values; since the reaction was carried at a pH value of approximately 12 the lignin precipitated shows a very dark color [106]. Second, the change of density can be explained by the elimination of less dense noncellulosic components due to the alkaline treatment [81].The slurry was washed several times by using a crystal column with a glass filter; the column needs to be shaken approximately every 10 minutes to facilitate the filtration process because of the high density of the slurry. When the slurry started to look of a lighter color, such as brown colored and the pH of the filtrated water was reduced



to approximately 10, the last washings were performed with lightly acidified water with a pH of approximately 6 till neutralization.

### 4.1.2 Bleaching treatment

The obtained material from the first step was put in reaction with an aqueous solution of acetic acid and sodium chlorite to perform the sodium chlorite oxidation treatment. Initially, the solution is of a light brown color, and with the progress of delignification by lignin oxidation, the color of the acid chloride solution becomes bright yellow [107]. This reaction was carried up at a fume hood because acetic acid and sodium chlorite produce chlorine dioxide and chloric and hydrochloric acids [108]. Chlorine dioxide is a yellow to reddish-yellow gas that is toxic by inhalation of critical concentration [109]. Two hours of reaction were enough for the complete whiteness of the cellulosic product, its necessary to mention that after one hour, an additional portion of sodium chlorite was added to reach the final product. The obtained cellulose was washed several times by using a glass column with a glass filter to filtrate the wastewater; the washings were repeated until the wastewater got neutral pH. Finally, the cellulose was washed by centrifugation 3 times, obtaining a clean white and dense product (Fig. 4.1 ,a and b). The cellulose was drying overnight at 45°C in ceramic capsules, getting dry completely white fibers with high crystallinity (Fig. 4.1 ,c).

High crystallinity of cellulose was proved by XRD presented in Fig.4.2, which shows one medium and broad peak at a  $2\theta$  value of  $15.9^\circ$ , one strong and sharp peak at  $22.2^\circ$ , and one weak peak at  $34.9^\circ$ . According to the literature [110], the signals that appear at  $2\theta = 22^\circ$  correspond to the crystallographic plane (002), the signal at  $15^\circ$  is attributed to the plane (101), the signal at  $16^\circ$  is assigned to the plane (10 $\bar{1}$ ), the signal at  $20.5^\circ$  corresponds to (020) plane. Finally, the signal at  $35^\circ$  is due to the plane (040). These planes are characteristic of cellulose type I. Extra sharp peaks are due to sample holder. The CI% was obtain as 86,46, with a  $I_{002}$  of 22460 and  $I_{AM}$  of 3040. Fig 4.3 shows the FTIR spectrum of the extracted cellulose from CPH. The spectrum shows the characteristic bands for the cellulose structure, which are represented in Table 4.1.

## 4.2 Carboxymethylation

The degree of substitution of sodium carboxymethyl cellulose is shown to be highly dependent on four different factors: etherification time, etherification temperature, the concentration of MCA, and NaOH concentration [11].

TABLE 4.1: FTIR vibrational bands of isolated CPH cellulose. Symbols meaning: w=weak, vw = very weak, sh = shoulder, s=strong, vs = very strong,  $\nu$  = stretching,  $\delta$  = bending,  $\omega$ =wagging,  $\rho$ =rocking, as= asymmetric, and s= symmetric, ip= In-plane.

$\lambda$ (cm <sup>-1</sup> )	Intensity	Vibration type	Assign
3331	s	$\nu$ O-H	Hydroxyl group, intra- and intermolecular hydrogen bond [79],[111–113]
2898	m	$\nu$ C-H (sp <sup>3</sup> )	Methylene group, C-H and CH <sub>2</sub> [79],[111–113]
1633	w	$\delta$ O-H	Absorbed water (hydrogen bonded) [79], [112–114]
1427	w	$\delta_s$ C – H <sub>2</sub>	CH <sub>2</sub> symmetric bending (scissoring) at C <sub>6</sub> [113], [115–118]
1367	w	$\delta$ C-H	Bending vibration of C-H and CH <sub>2</sub> groups [118]
1316	w	$\omega, \rho$ C – H <sub>2</sub>	C – H <sub>2</sub> Wagging at C <sub>6</sub> Hydroxyl group or C – H <sub>2</sub> rocking vibration [119]
1268	w	$\omega$ C-H	CH wagging vibration [119]
1202	w	$\delta_{ip}$ CO-H	CO-H in-plane at C <sub>6</sub> [118]
1159-1025	m to vs.	$\nu$ C-O	C-O-C pyranose ring stretching [79, 119]
896	m	$\nu$ C-O-C	C-O-C at $\beta$ glycosidic linkage amorphous region [111, 119]

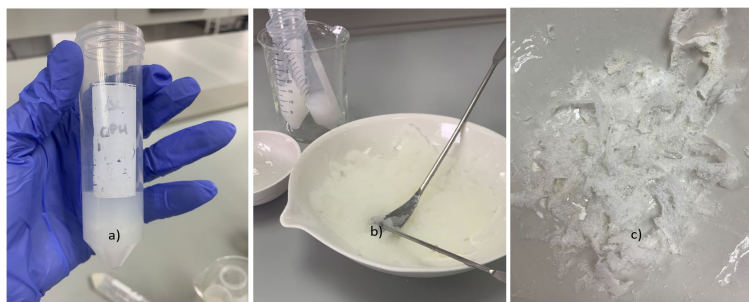


FIGURE 4.1: Pure cellulose, a) centrifuged, b) In ceramic capsule, c) dry

### 4.2.1 Synthesis 1

Three different syntheses were made by varying variables based on previously reported works. The first synthesis was made with a high concentration hydroxide solution similar to [83] (50 % NaOH aqueous solution), the amount of monochloroacetic acid proposed by [95], and an etherification temperature of  $75^{\circ}\text{C}$ . The obtained product has a weight of 5.01 g, representing a 501% yield concerning cellulose reactant. Since NaCMC synthesis is a 1:1 reaction with cellulose, this kind of yield shows a high quantity of by-product contaminants. Observing the mother liquor from the filtration of the carboxymethylation reaction makes it easy to recognize the presence of tiny crystals that can be NaCl crystals. The product also has the presence of sodium glycolate produced by the side reaction. A proof of solubility was made by preparing a 2% product-water solution; the solution shows low viscosity and high turbidity after 3h of agitation and does not form any film after drying. However, based on the yield and the fact that NaCMC is formed in a 1: 1 reaction with cellulose, a 10% product-water solution was prepared; this mixture, in theory, should represent a 2% NaCMC- water solution. The solution presents a little viscosity and continues showing turbidity after 3h agitation at 400rpm and room temperature. The solution was dry in a small polyethylene capsule at  $45^{\circ}\text{C}$ , forming a thin white film difficult to extract from the capsule without breaking Fig.4.7.a.

The Fig 4.4 show FTIR spectra of NaCMC1. Principal spectrum bands are detailed in Table 4.2 NaCMC shares some functional groups with cellulose that are presented at the IR as a free hydroxyl group ( $-\text{OH}$  stretching) near  $3300\text{ cm}^{-1}$ , a hydrocarbon group ( $\text{C-H}$  stretching) near  $2895\text{ cm}^{-1}$ , a  $-\text{CH}_2$  scissoring around  $1420\text{ cm}^{-1}$ , an  $-\text{OH}$  in plane bending vibration around  $1320\text{ cm}^{-1}$ , and ether groups ( $-\text{O}-$  stretching) near  $1010\text{ cm}^{-1}$  [115]. The bands present between  $800$  and  $500\text{ cm}^{-1}$  are related to heavy atom flexing in both  $\text{C-O}$  and ring vibrational modes, with a contribution of ring stretching [83]. The introduction of a  $-\text{OCH}_2\text{COO}-$  group into the cellulose molecule is confirmed by the presence of an intense bands around  $1595$

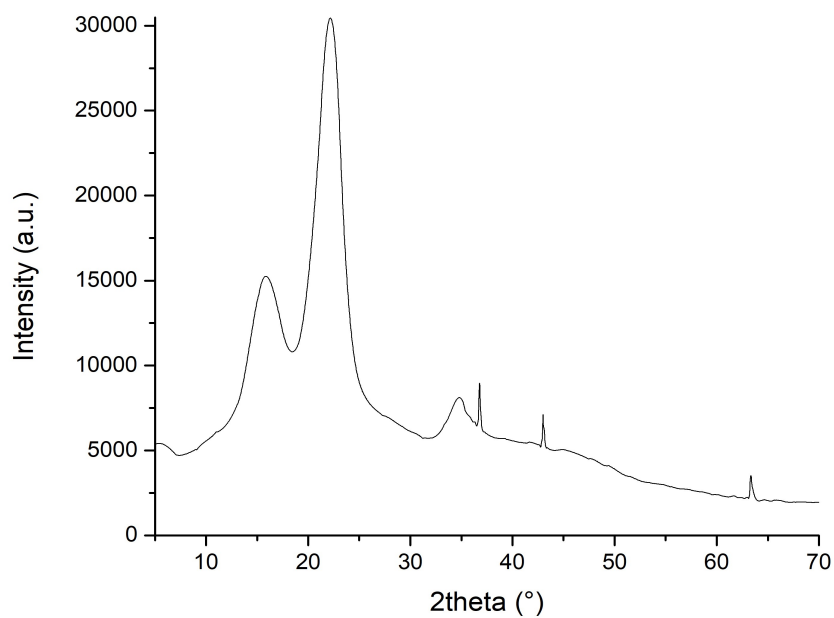


FIGURE 4.2: X-ray Diffraction pattern of CPH-Cellulose.

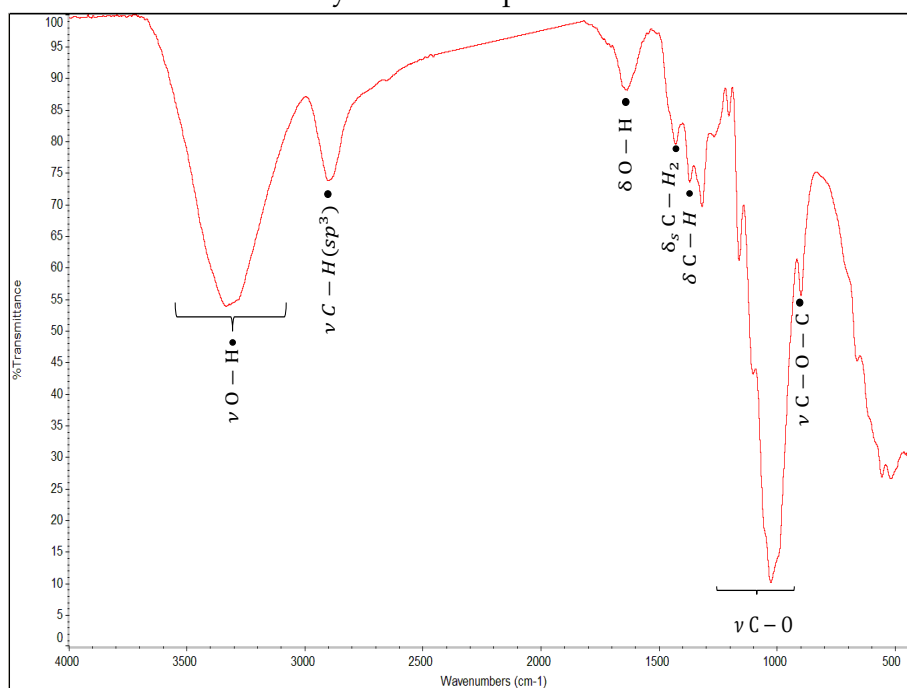


FIGURE 4.3: FTIR spectra of extracted CPH cellulose.

$\text{cm}^{-1}$  and the increase of intensity of the band at approximate  $1413 \text{ cm}^{-1}$ , which correspond to asymmetric and symmetric stretching vibrations of the carboxylate group. In addition, an increase in the ether peak  $-\text{CH}_2-\text{O}-\text{CH}_2-$  group stretching vibration near  $1060 \text{ cm}^{-1}$  is complementary to the confirmation [83, 94, 115]. The strong  $\text{C}=\text{O}$  peak for the NaCMC product is related to a large extent of etherification. In addition, the lowered intensity at  $-\text{OH}$  peak, suggests a high replacement of hydroxyl groups in the cellulose molecule with carboxymethyl groups in the NaCMC products, the product of the reaction with the etherifying agent [94, 96]. Principal spectrum bands are detailed at the Table 4.2.

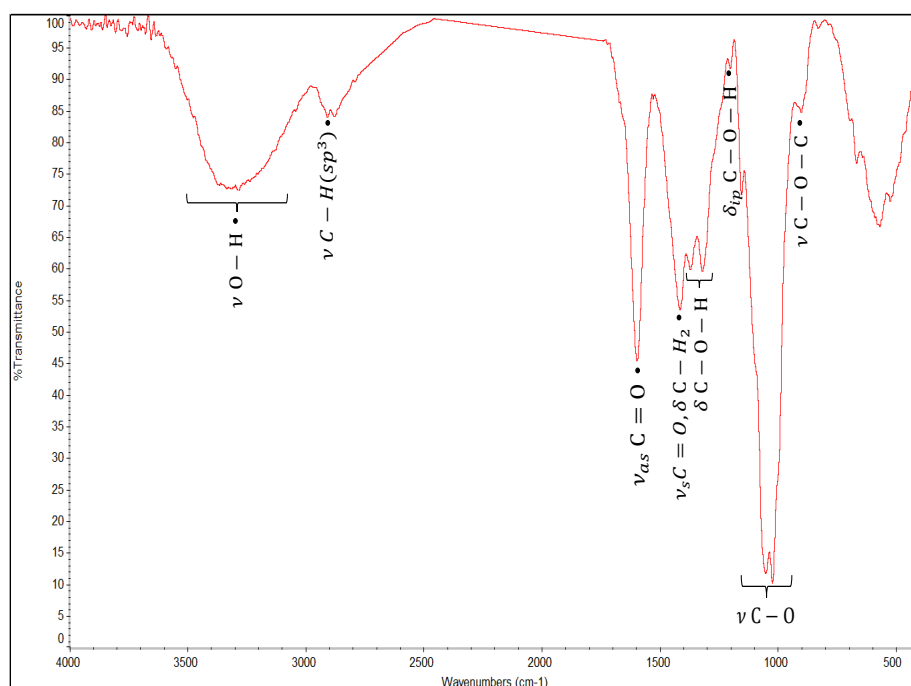


FIGURE 4.4: FTIR spectra of NaCMC1.

### 4.2.2 Synthesis 2

For the second synthesis, the concentration of NaOH was change by using 10% NaOH(w/w %) solution, also the quantity of monochloroacetic acid was changed to 2,76 g per gram of cellulose, the time of the etherification reaction was increase to 3.5 h and the organic solvent used was ethanol. The reaction temperature was kept at  $75^{\circ}\text{C}$ . As a result of this reaction, a total of 1.107 g of dry product was obtained, this quantity represents a yield of 110. 79%. Since cellulose produces NaCMC in a 1:1 reaction, this yield can give an idea of the low formation of sub-products. Solubility was analyzed by making a 2% solution and letting this solution under agitation at room temperature for 3h. After 3h was observed a medium viscous solution that

TABLE 4.2: FTIR vibrational bands of NaCMC1. Symbols meaning: w=weak, vw = very weak, sh = shoulder, s=strong, vs = very strong,  $\nu$  = stretching,  $\delta$  = bending, as= asymmetric, and s= symmetric.

$\lambda$ (cm <sup>-1</sup> )	Intensity	Vibration type	Assign
3281	m	$\nu$ O-H	Hydroxyl group, intra-and intermolecular hydrogen bond [82, 83, 94, 112, 113, 115, 120]
2906-2877	m	$\nu$ C-H (sp <sup>3</sup> )	Methylene group, CH and CH <sub>2</sub> [113, 115, 120, 121]
1595	s	$\nu_{as}$ C=O	COO <sup>-</sup> Asymmetric stretch [83, 94, 96, 112, 113, 115, 120, 121]
1413	s	$\nu_s$ C=O, $\delta$ C-H <sub>2</sub>	COO <sup>-</sup> Symmetric stretch Carboxylate salt [83, 89, 118, 120, 121], methylene group, CH and CH <sub>2</sub> [113, 115-118]
1369-1319	m	$\delta$ C-O-H	Hydroxyl group, C-OH bending vibration [83, 113-116, 118]
1202	w	$\delta_{ip}$ CO-H	CO-H in-plane at C <sub>6</sub> [118]
1153-1022	m to vs.	$\nu$ C-O	C-O-C pyranose ring stretching [79, 119]
896	m	$\nu$ C-O-C	C-O-C at $\beta$ glycosidic linkage amorphous region [111, 119]
800-500	m		Heavy atom flexing in both C-O and ring vibrational modes, with a contribution of ring stretching [83]

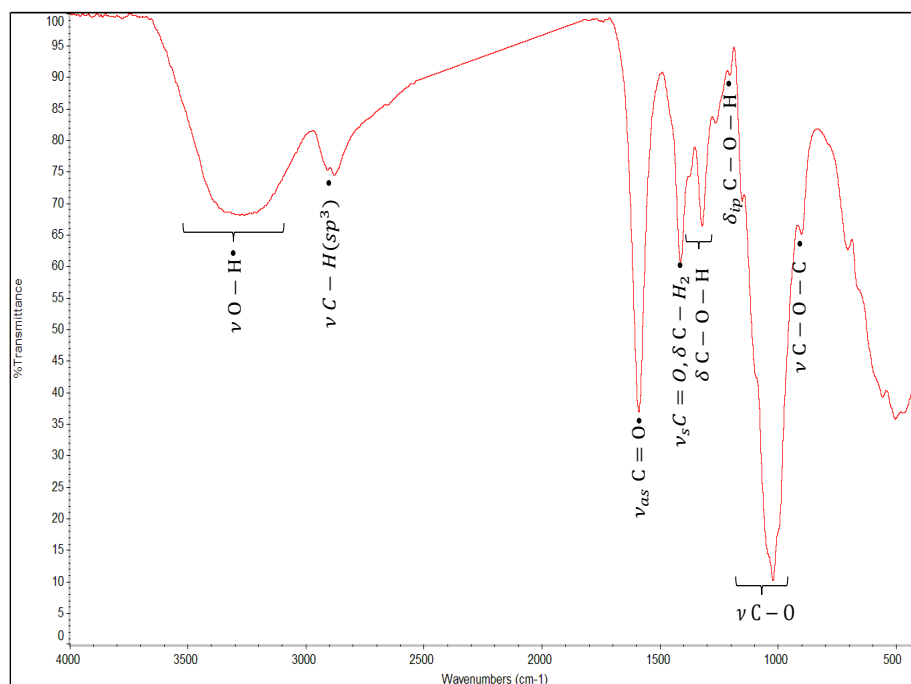


FIGURE 4.5: FTIR spectra of NaCMC2.

was put to dry overnight in a polyethylene capsule at 45<sup>0</sup>C. The next day a thin and brittle film was obtained; this film was covered with residues that do not let any transparency be observed Fig. 4.7.b. So, this product needs to pass through a purification procedure to be used for the formation of a transparent hydrogel. The formation of NaCMC was again evaluated by FTIR spectroscopy Fig.4.5. that shows the formation of the objective product by the presence of characteristic bands, that include strong bands at 1584 and 1410 cm<sup>-1</sup> that represent the asymmetric and symmetric stretching vibration of C=O of the carboxylate group and its salt, that confirm the substitution of carboxymethyl groups in cellulose structure[83, 122]. Additionally, the reduction of intensity of the O-H stretching band and the increase of intensity C=O stretching band are representative of a high extent of substitution [94, 122]. Principal spectrum bands are detailed at the Table 4.2.

### 4.2.3 Synthesis 3

For the third and last synthesis, the NaOH concentration of NaOH varied to 4.87% NaOH(w/w %) in solution, also the temperature of the etherification reaction was controlled between 68 and 70<sup>0</sup>C, and the reaction time of etherification reaction was 1.5h. The amount of monochloroacetic acid was 1.6 g per gram of cellulose, the same as that for the first synthesis. The obtained product has a yield of 109.5%. The control of the temperature close but always lower than 70<sup>0</sup>C was determined crucially

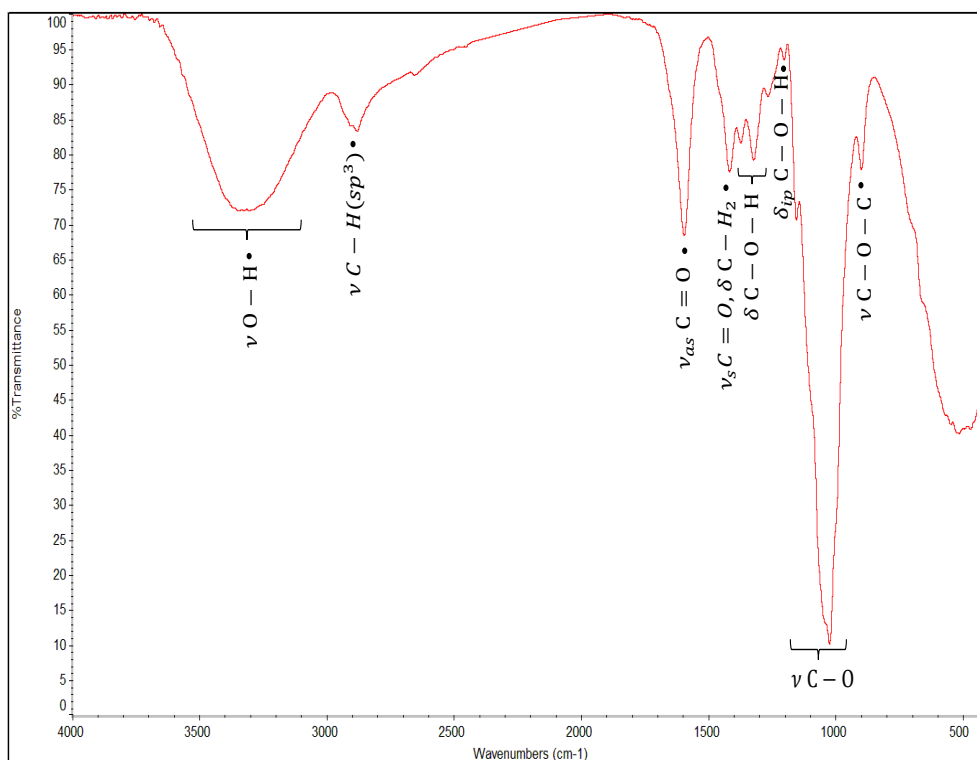


FIGURE 4.6: FTIR spectra of NaCMC3.

by the previous work of Chen et al., 2020 because high temperature increased the swelling speed of the cellulose and facilitated the permeation of MCA, but at temperatures higher than 70°C the DS is lowered. The time of reaction of etherification reaction needs to be enough, but it also is required to take into account that a too long etherification time can aggravate the production of the subproducts and degrade NaCMC by oxygen degradation[96]. Also, the concentration of MCA needs to be fixed to have good availability of acidic molecules, but an excess of MCA could increase the production of subproducts. Rachtanapun et al. (2021) determined 1.6 g of MCA per gram of cellulose is an optimal quantity for the production of NaCMC with a high DS value [95]. The solubility was analyzed by making a 2% solution and letting this solution under agitation at room temperature for 3h. The result of this mixture was very viscous after 3h and less cloudy than the previously synthesized NaCMC. The mixture was let to dry in a polyethylene capsule overnight; the next day, obtaining a film that was easy to separate from the capsule, but the solid was excessive and did not let to show any transparency, so a purification reaction was considered (Fig 4.7.c). NaCMC formation was confirmed by the FTIR spectroscopy (Fig 4.6), confirming the presence of NaCMC by the presence of medium bands at 1594 and 1415  $\text{cm}^{-1}$ , which represent the asymmetric and symmetric stretching vibration of C=O of the carboxylate group and its salt, and confirm the substitution



of carboxymethyl groups in cellulose structure[83, 122]. Additionally, the reduction of intensity of the O-H stretching band and the increase of intensity C=O stretching band are representative of a high extent of substitution [94, 122]. Principal spectrum peaks are detailed at the Table 4.2.

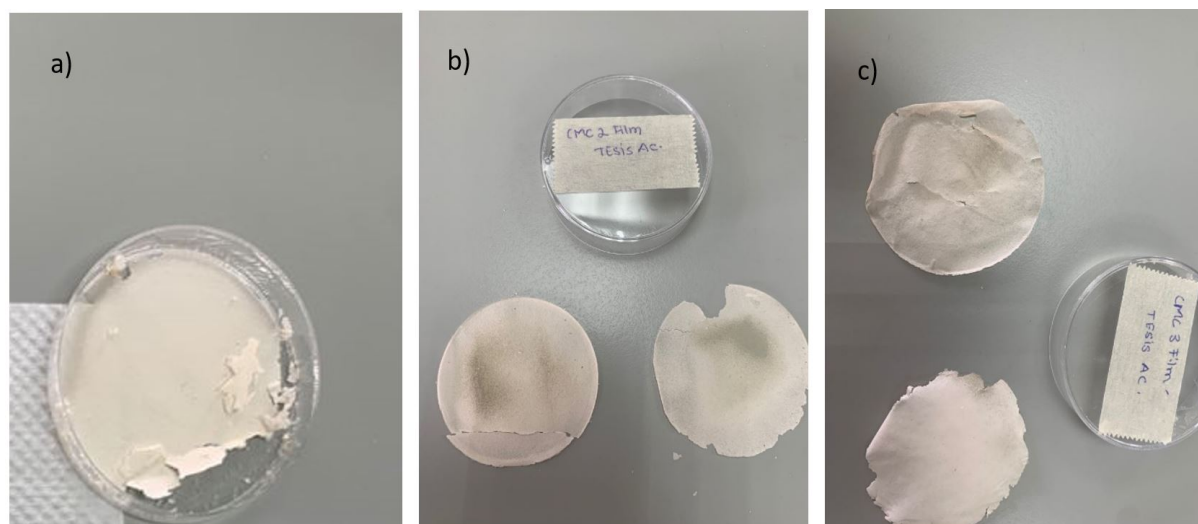


FIGURE 4.7: NaCMC water dilution after drying.(a) NaCMC1, (b) NaCMC2, (c) NaCMC3.

### 4.3 Purification

The purification of NaCMC is based on the difference in solubilities of the sub-products and the target product. The solubility of NaCMC was changed by reaction with sulfuric acid, changing NaCMC from its sodium salt to its free acid form (HCMC). HCMC precipitates when sodium carboxymethylcellulose reacts in an acidified aqueous solution with a pH of 2 or less [123]. While HCMC is formed, the sub-products are changed by reaction with acid to highly water-soluble molecules glycolic acid (Fig 4.8) , sodium sulfate, and hydrochloric acid Fig (4.9) . After reaction time was complete, these highly water-soluble subproducts were separated by filtration; also a series of washings with water was performed to be sure of eliminating all the subproducts, till very low cloudiness was observed in the mother liquor. As a second step, the neutralization of the HCMC to recover the sodium salt was performed by using an ethanolic solution of sodium hydroxide. After reaction time, the product was filtered and washed several times with ethanol till neutralization of the product; this guarantees the removal of alkali excess (purification).The final yield after purification was 54.60% for NaCMC1, 80.13% for NaCMC2, and 68.07%

for NaCMC3. FTIR of the purified products was obtained to confirm the conservation of the NaCMC products. The presence of bands near 1600 and 1420  $\text{cm}^{-1}$  represent the asymmetric and symmetric stretching vibration of C=O, of the carboxylate group and its salt, that confirm the presence of the target product[83, 122]. Purified NaCMC1 presents medium bands at 1592 and 1418  $\text{cm}^{-1}$  (Fig 4.11), purified NaCMC2 presents strong bands at 1592 and 1413  $\text{cm}^{-1}$  (Fig 4.12), and purified NaCMC3 presents strong bands at 1592 and 1425  $\text{cm}^{-1}$  (Fig 4.6). The increase of intensities of purified NaCMC3 represents a high extent of substitution at the target product[94, 122]. Principal spectrum bands of purified samples are detailed in table 4.3. The solubility of the purified NaCMC from the different syntheses was analyzed by preparing 1ml of 2% (w/w) NaCMC: water solution. The NaCMC2 and NaCMC3 show high viscosity and transparency after 3h of stirring at room temperature. NaCMC1 solution was less viscous and a little cloudy. The three solutions were dry overnight to examine the formation of films, NaCMC1 and NaCMC2 give highly transparent films and because of this, both products were selected for the formation of the hydrogels Fig. 4.10.

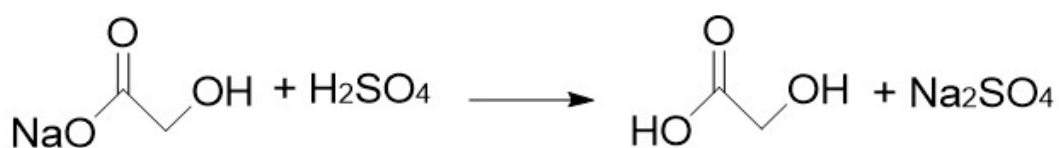


FIGURE 4.8: Glycolic acid formation reaction.



FIGURE 4.9: Sodium Sulfate formation reaction.

## 4.4 Phenolic compounds

The efficacy of the phenolic extract of CPH as an antioxidant was examined in previous work, and the solvent election was selected based on this work as 80% ethanol solution [28]. The extraction was performed by a three-day maceration under dark conditions to prevent any degradation, and the resulting liquid after filtration was yellow-colored with light brown coloration. The presence of phenols and polyphenols was confirmed by having positive results in the five phytochemical tests performed on the extract (Table 4.4 and Fig 4.14). Also quantification of the concentration of the phenols was obtained by Folin–Ciocalteu (F–C) assay at three different

TABLE 4.3: FTIR vibrational bands of purified NaCMC1. Symbols meaning: w=weak, vw = very weak, sh = shoulder, s=strong, vs = very strong,  $\nu$  = stretching,  $\delta$  = bending, as= asymmetric, and s= symmetric.

$\lambda(\text{cm}^{-1})$	Intensity	Vibration type	Assign
3346	m	$\nu$ O-H	Hydroxyl group, intramolecular hydrogen bond [82, 83, 94, 112, 113, 115, 120]
2904	m	$\nu$ O-H	Hydroxyl group, carboxylate [82]
2878	m	$\nu$ C-H ( $\text{sp}^3$ )	Methylene group, CH and CH <sub>2</sub> [113, 115, 120, 121]
1648	w	$\delta$ O-H	Absorbed water [79, 112–114]
1592	s	$\nu_{as}$ C=O	COO <sup>-</sup> Asymmetric stretch [83, 94, 96, 112, 113, 115, 120, 121]
1418	s	$\nu_s$ C=O, $\delta$ C-H <sub>2</sub>	COO <sup>-</sup> Symmetric stretch Carboxylate salt [83, 89, 118, 120, 121], methylene group, CH and CH <sub>2</sub> [113, 115–118]
1367	m	$\delta$ C-O-H	Hydroxyl group, C-OH bending vibration [83, 113, 115, 118]
1319	m	$\delta$ CO-H	Hydroxyl group [114, 116, 118]
1267	w	$\omega$ C-H	Wagging of CH [119]
1202	w	$\delta_{ip}$ CO-H	CO-H in-plane at C <sub>6</sub> [118]
1153-995	m to vs.	$\nu$ C-O	C-O-C pyranose ring stretching [79, 119]
896	m	$\nu$ C-O-C	C-O-C at $\beta$ glycosidic linkage amorphous region [111, 119]
800-500	s		Heavy atom flexing in both C-O and ring vibrational modes, with a contribution of ring stretching [83]

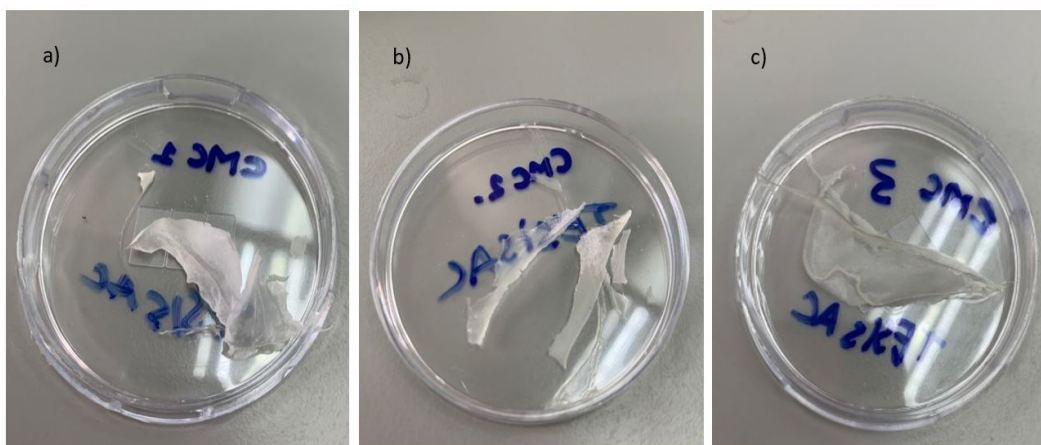


FIGURE 4.10: Purified NaCMC dilution test.

dilutions. All the statistical data was obtained by using the Origin Pro program. The linear fit is present in Fig.4.15 and shows that the line of best fit is described by the equation  $y = 6.38127 + 0.00239x$ . Linear adjustment shows to fit almost perfectly all the plotted points, also R-square was determined as 0.9997 that is very close to 1, and shows a good linear adjustment. The residuals plot in Fig.4.17 does not show any tendency, which is associated with a satisfactory distribution of residuals. In the same way in the graph of the confidence limits Fig.4.16, the hyperbolas show to be close to the adjusted line what is associated with small errors in the determination of concentration values[124]. The average total phenolic concentration obtained by the interpolation is  $0.6656 \pm 0.0344$  mg GAE/mL of phenolic extract or 13.3126 mg GAE/g of dry CPH sample, Table 4.5. The concentration value is reported with the estimated standard deviation of the concentration  $S_{x_0}$ , which is a little bigger than the standard deviation of about 0.0333. The data associated with the calculus of errors at Folin–Ciocalteu assay are present in Appendix A.

## 4.5 Hydrogel preparation

Hydrogels were prepared by the mixture of NaCMC with water, citric acid that is a non-toxic crosslinking agent, and the phenolic extract of the CPH phenolics. Previous work shows that phenolics enhanced the gelation behavior by acting as physical crosslinking agents through inter-hydrogen bonds with polymeric chains [125]. Films were first prepared by using commercial NaCMC to detect which concentration of phenolic extract gives better performance. Films were prepared with 5,10, 15, and 20% of phenolic extract. The mixture was let under string for 3 hours, obtaining gels with different viscosity; the viscosity increases with the phenolic extract

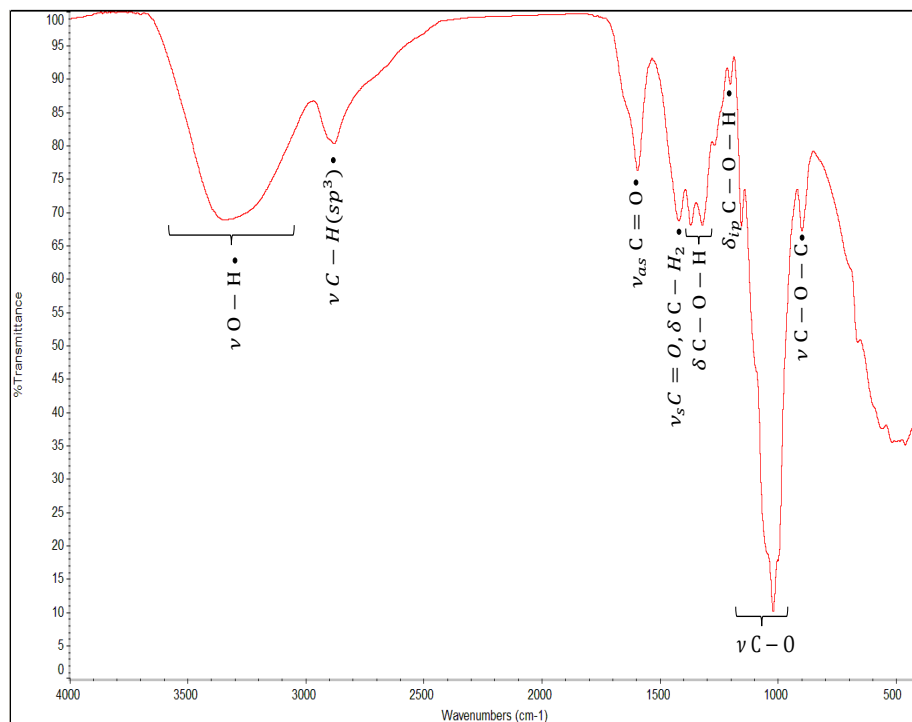


FIGURE 4.11: FTIR spectra of purified NaCMC1.

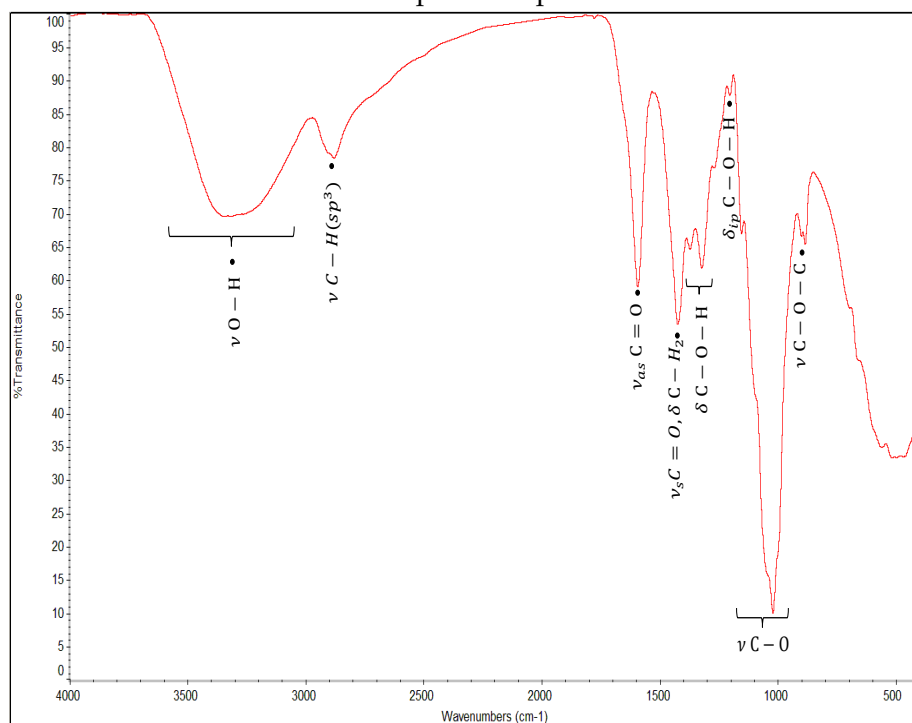


FIGURE 4.12: FTIR spectra of purified NaCMC2.

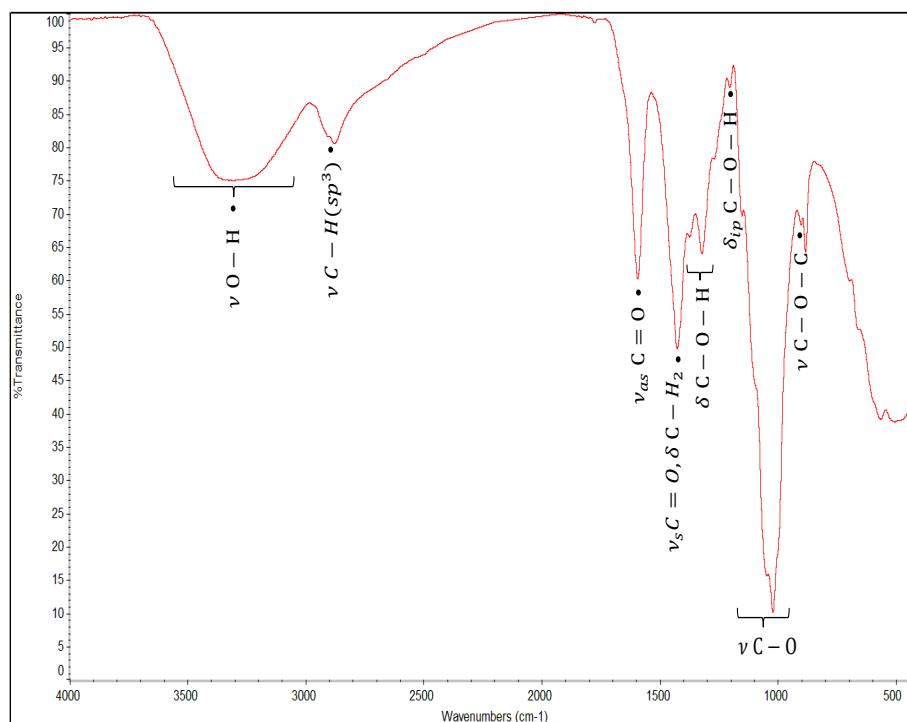


FIGURE 4.13: FTIR spectra of purified NaCMC3.

concentration. The hydrogels were allowed to dry overnight at 45<sup>0</sup>C to form a thin hydrogels film. Hydrogel films preparation and evaluation were repeated to observe the repeatability of the experiment. The UV blocking activity was evaluated by measuring its transmittance by using a solid UV VIS spectrophotometer. The different transmittance profiles are presented in Fig.4.18 , and for the repeated test in Fig.4.19. The result of this test is that the UV blocking profile increase with the increase of phenolic concentration, the obtained values at the extremes of UVA (320-400 nm) and UVB (290-320 nm) ranges are present in Table 4.6 for films prepared with 5% of phenolic extract, Table 4.7 for 10% of phenolic extract, Table 4.8 for 15% of phenolic extract and Table 4.9 for 20% of phenolic extracts. Results of both test samples shows that the best UV protecting activity is for the films with 20% of phenolic extract. Blank material without phenolic extract was prepared to prove that UV protective activity is directly related to the presence of phenolic extract Table 4.10. Once these good UV blocking profile results were obtained, the efficacy of the target product was tested. Hydrogel films were prepared with NaCMC2 and NaCMC3, and a test gel was prepared with NaCMC3 without adding the crosslinked agent. The UV-Vis profiles show incredible results for the three films, the best profile was obtained for the test gel with average transmittances of (0.98± 0.39)%T at 290nm, (3. 59±1.01)%T at 320 nm, and (29. 71±1.95)%T at 400nm , these wavelengths comprises the extremes of the UVA and UVB test. Good results were also obtained

TABLE 4.4: Phytochemical test results.

Phytochemical components	Test	Observation	Inference
Phenol	Ferric Chloride	Bluish black colour	+
	Ellagic acid	Brown color, with a little brown precipitate	+
Flavonoids	Alkaline test	Deep yellow color	+
	Shinoda test	Crimson red coloration	+
Tannins	Ferric Chloride	Deep green precipitate	+

TABLE 4.5: Phenolic concentration determination by F-C assay

Dilution factor	Absorbance	Diluted concentration (mg GAE/mL of extract)	Concentration (mg GAE/mL of extract)
1:10	0.064	0.06435	0.6435
1:20	0.035	0.03520	0.7040
1:40	0.015	0.01624	0.6495
		Average	0.6656±0.0344

for the NaCMC2 and NaCMC3 films. In the case of NaCMC2 film gives average transmittances of (34.13±2.69)%T at 290nm, (52.12±1.57)%T at 320 nm, and (75.57±0.47)%T at 400nm. Finally, NaCMC3 film gives average transmittances of (11.60±0.84)%T at 290nm, (32.36±1.30)%T at 320 nm, and (79.37±0.42)%T at 400nm. The transmittance results are presented in Fig 4.20 and Table 4.11 and 4.12. The average transmittance values are reported with the corresponding standard deviation values. Additionally, films formed with citric acid were very flexible and transparent, even though NaCMC2 shows a small number of impurities on its surface. The test film is very transparent and presents a light brown coloration but is slightly flexible. Fig 4.21, show the different films formed with 20 % of phenolic extract in solution. Fig. 4.22, shows the flexibility, transparency, and gelation behavior of NaCMC3 hydrogel formed with 20 % of phenolic extract and citric acid. The FTIR spectroscopy of the films was performed, showing alteration of the NaCMC profile for the ones that were prepared in presence of the crosslinking agent. For NaCMC3 film FTIR spectra (Fig 4.23) the appearance of two bands attributed to the carbonyl stretching vibration, one band at 1742 cm<sup>-1</sup> (ester carbonyl) and one extra band at 1589 cm<sup>-1</sup> (carboxylate), confirm the presence of the ester formed during crosslinking [89]. NaCMC2 film presents the same characteristic bands at 1708 and 1579 cm<sup>-1</sup>

(Fig 4.24). Detailed FTIR bands for NaCMC2 and NaCMC3 film are present in the Table. 4.13. On the other hand, NaCMC3 film formed without citric acid crosslinker lacks the presence of ester carbonyl stretching vibration (Fig 4.25 and Table 4.14).

The selection of the best product depends on the application in which go to be used, NaCMC3 film prepared by crosslinking with citric acid produces highly flexible hydrogel film, which is a good option to be used for the preparation of facial masks with high antioxidant activity of CPH phenolic extract, reported on literature. On the other side, if the objective is to apply the gel directly on the skin for UV protection NaCMC3 gel prepared without citric acid offers a light texture that can be more easily absorbed by the skin, and also show greater protection against UVA and UVB.

The followed conclusions and recommendation chapter present the different inferences made after analyzing the results of the experimental work, the personal experience at the laboratory work, and the correlation with different bibliographic sources presented in both the theoretical framework and the present chapter.



TABLE 4.6: Test films with commercial NaCMC at 5% phenolic extract. Transmittance values at UVA and UVB extremes.

$\lambda$	5% Film Test 1			5% Film Test 2		
	290	320	400	290	320	400
	50.11	68.82	87.50	56.31	72.31	87.58
	42.86	64.11	86.62	58.97	73.62	87.86
$\%T$	$46.49 \pm 5.12$	$66.46 \pm 3.33$	$87.06 \pm 0.63$	$57.64 \pm 1.87$	$72.97 \pm 0.92$	$87.72 \pm 0.19$

TABLE 4.7: Test films with commercial NaCMC at 10% phenolic extract. Transmittance values at UVA and UVB extremes.

$\lambda$	10% Film Test 1			10% Film Test 2		
	290	320	400	290	320	400
	43.44	64.80	85.80	40.80	61.89	85.72
	40.65	62.97	86.10	40.09	61.12	85.61
$\%T$	$42.05 \pm 1.97$	$63.88 \pm 1.30$	$85.95 \pm 0.21$	$40.45 \pm 0.51$	$61.50 \pm 0.54$	$85.66 \pm 0.08$

TABLE 4.8: Test films with commercial NaCMC at 15% phenolic extract. Transmittance values at UVA and UVB extremes.

$\lambda$	15% Film Test 1			15% Film Test 2		
	290	320	400	290	320	400
	10.64	32.40	78.11	33.78	55.81	84.76
	13.01	35.95	79.40	33.95	56.07	84.78
$\%T$	$11.82 \pm 1.67$	$34.17 \pm 2.51$	$78.75 \pm 0.91$	$33.87 \pm 0.12$	$55.94 \pm 0.18$	$84.77 \pm 0.01$

TABLE 4.9: Test films with commercial NaCMC at 20% phenolic extract. Transmittance values at UVA and UVB extremes.

$\lambda$	20% Film Test 1			20% Film Test 2		
	290	320	400	290	320	400
	10.51	31.05	74.70	13.70	34.49	80.28
	13.00	34.97	75.56	12.49	32.46	79.32
$\%T$	$11.76 \pm 1.75$	$33.01 \pm 2.77$	$75.13 \pm 0.61$	$13.10 \pm 0.85$	$33.48 \pm 1.43$	$79.80 \pm 0.68$

TABLE 4.10: Test films with commercial NaCMC blank. Transmittance values at UVA and UVB extremes.

		Blank		
$\lambda$	290	320	400	
	73.82	81.48	89.32	
	75.39	82.39	89.32	
$\% \bar{T}$	$74.61 \pm 0.61$	$81.94 \pm 1.11$	$89.32 \pm 0.64$	

TABLE 4.11: CPH-NaCMC2 film with 20 percent of phenolic extract. Transmittance values at UVA and UVB extremes.

		CMC2 film		
$\lambda$	290	320	400	
	31.18	50.50	75.33	
	36.46	53.63	76.11	
	34.75	52.22	75.28	
$\% \bar{T}$	$34.13 \pm 2.69$	$52.12 \pm 1.57$	$75.57 \pm 0.47$	

TABLE 4.12: CPH-NaCMC3 films with 20 percent of phenolic extract. Transmittance values at UVA and UVB extremes.

		NaCMC3 film			NaCMC3 film without citric acid		
$\lambda$	290	320	400	290	320	400	
	10.68	31.43	79.15	0.75	4.76	28.83	
	11.79	31.80	79.86	0.76	2.97	31.95	
	12.33	33.85	79.12	1.44	3.05	28.35	
$\% \bar{T}$	$11.60 \pm 0.84$	$32.36 \pm 1.30$	$79.38 \pm 0.42$	$0.98 \pm 0.39$	$3.59 \pm 1.01$	$29.71 \pm 1.95$	

TABLE 4.13: FTIR vibrational bands of NaCMC3 film. Symbols meaning: w=weak, vw = very weak, sh = shoulder, s=strong, vs = very strong,  $\nu$  = stretching,  $\delta$  = bending, as= asymmetric, and s= symmetric.

$\lambda$ ( $\text{cm}^{-1}$ )	Intensity	Vibration type	Assign
3381	m	$\nu$ O-H	Hydroxyl group, intramolecular hydrogen bond [82, 83, 94, 112, 113, 115, 120]
2926	m	$\nu$ C-H ( $\text{sp}^3$ )	Methylene group, CH and CH <sub>2</sub> [113, 115, 120, 121]
1708	vs	$\nu$ C=O	Ester carbonyl [89]
1578	s	$\nu_{as}$ C=O	COO <sup>-</sup> Asymmetric stretch [83, 89, 94, 96, 112, 113, 115, 120, 121]
1391	m	$\delta$ C-O-H	Hydroxyl group, C-OH bending vibration [83, 113, 115, 118]
1318	m	$\delta$ CO-H	Hydroxyl group [114, 116, 118]
1202	w	$\delta_{ip}$ CO-H	CO-H in-plane at C <sub>6</sub> [118]
1103-1021	m to vs.	$\nu$ C-O	C-O-C pyranose ring stretching [79, 119]
890	m	$\nu$ C-O-C	C-O-C at $\beta$ glycosidic linkage amorphous region [111, 119]
800-500	s		Heavy atom flexing in both C-O and ring vibrational modes, with a contribution of ring stretching [83]

TABLE 4.14: FTIR vibrational bands of NaCMC3 film without citric acid. Symbols meaning: w=weak, vw = very weak, sh = shoulder, s=strong, vs = very strong,  $\nu$  = stretching,  $\delta$  = bending, as= asymmetric, and s= symmetric.

$\lambda$ (cm <sup>-1</sup> )	Intensity	Vibration type	Assign
3277	m	$\nu$ O-H	Hydroxyl group, intramolecular hydrogen bond [82, 83, 94, 112, 113, 115, 120]
2921	m	$\nu$ O-H	Hydroxyl group, carboxylate [82]
2874	m	$\nu$ C-H (sp <sup>3</sup> )	Methylene group, CH and CH <sub>2</sub> [113, 115, 120, 121]
1591	s	$\nu_{as}$ C=O	COO <sup>-</sup> Asymmetric stretch [83, 94, 96, 112, 113, 115, 120, 121]
1406	s	$\nu_s$ C=O, $\delta$ C-H <sub>2</sub>	COO <sup>-</sup> Symmetric stretch Carboxylate salt [83, 89, 118, 120, 121], methylene group, CH and CH <sub>2</sub> [113, 115–118]
1364	m	$\delta$ C-O-H	Hydroxyl group, C-OH bending vibration [83, 113, 115, 118]
1319	m	$\delta$ CO-H	Hydroxyl group
1202	w	$\delta_{ip}$ CO-H	CO-H in-plane at C <sub>6</sub> [118]
1153-1018	m to vs.	$\nu$ C-O	C-O-C pyranose ring stretching [79, 119]
835	m	$\nu$ C-O-C	C-O-C at $\beta$ glycosidic linkage amorphous region [111, 119]
800-500	s		Heavy atom flexing in both C-O and ring vibrational modes, with a contribution of ring stretching [83]

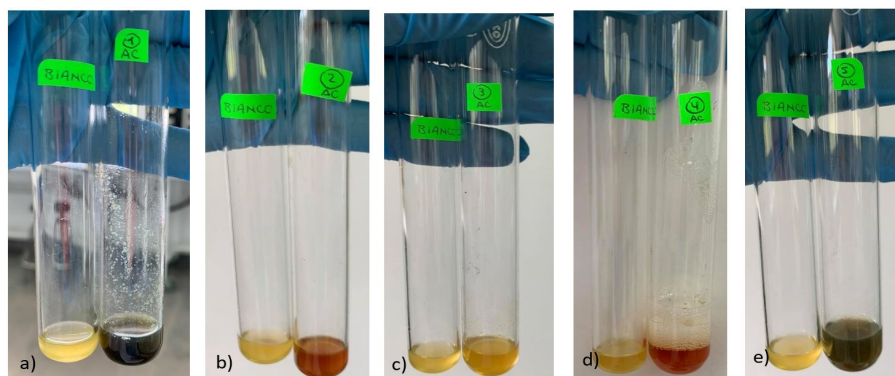


FIGURE 4.14: Phytochemical test. a) Ferric Chloride (Phenols), b) Ellagic acid (phenols), c) Alkaline test (flavonoids), d) Shinoda test (flavonoids), e) Ferric Chloride (tannins).

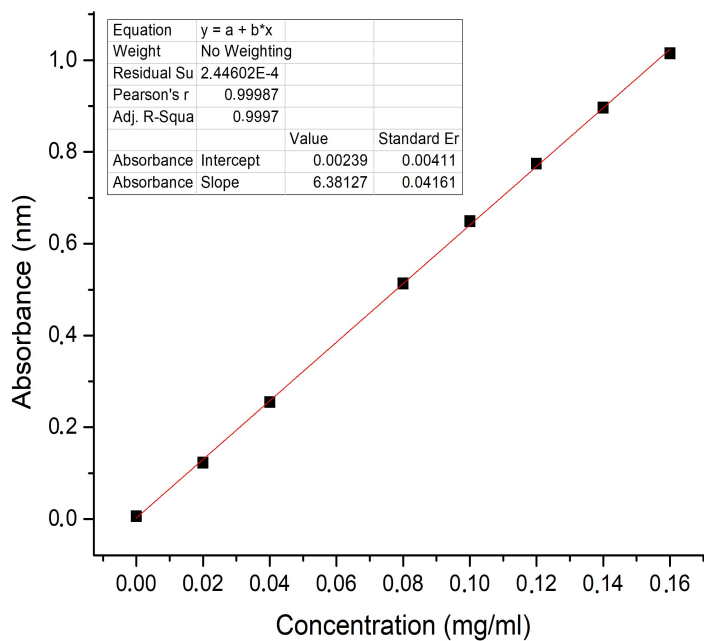


FIGURE 4.15: Linear regression of Folin-Ciocalteu (F-C) assay .

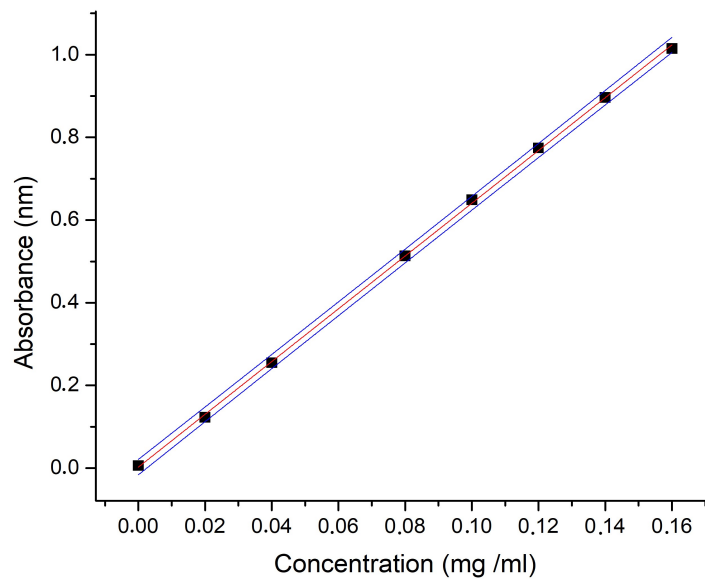


FIGURE 4.16: Linear regression of Folin-Ciocalteu (F-C) assay with confidence lines.

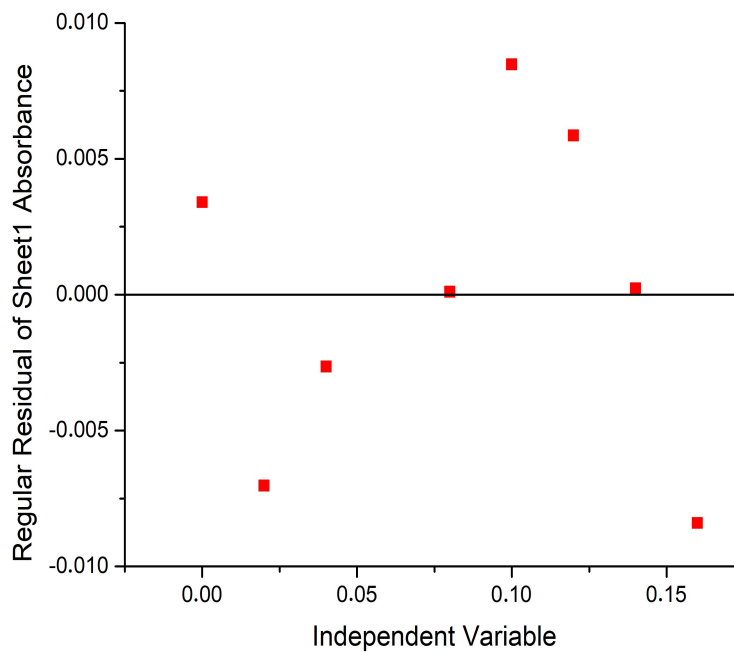


FIGURE 4.17: Graph of residuals of linear regression of Folin-Ciocalteu (F-C) assay .

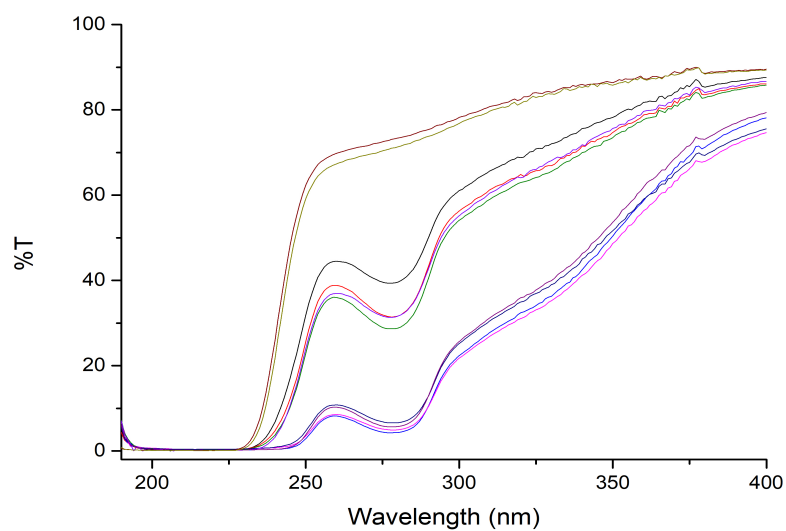


FIGURE 4.18: Transmittance plots of commercial NaCMC films test 1.

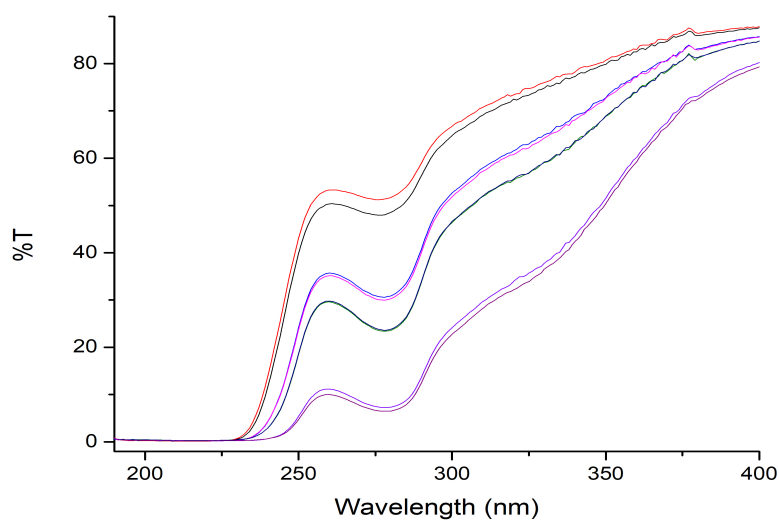


FIGURE 4.19: Transmittance plots of commercial NaCMC films test 2.

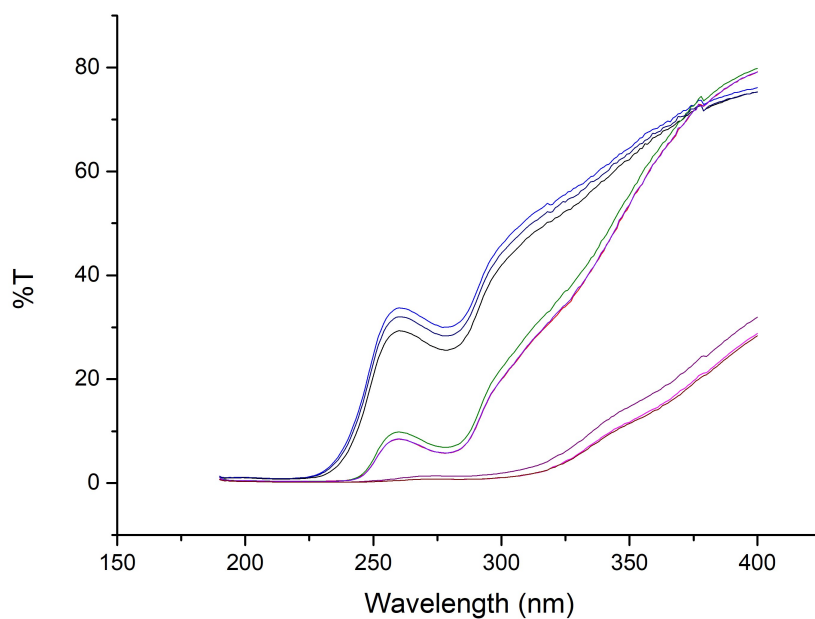


FIGURE 4.20: Transmittance profiles of CPH-CMC films.

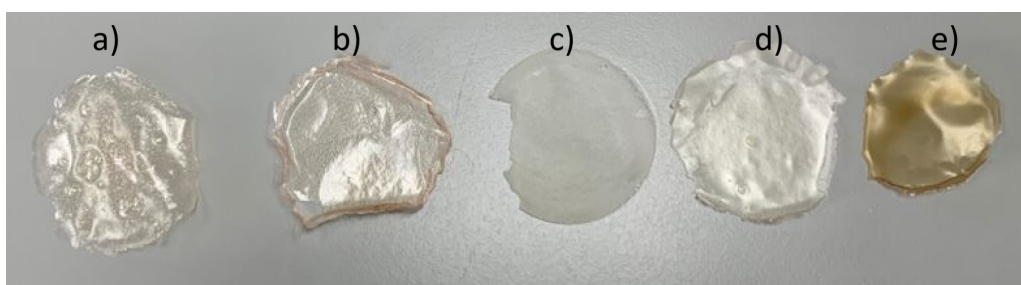


FIGURE 4.21: Films prepared with 20% of phenolic extract in solution. a) Commercial NaCMC film test 1, b) commercial NaCMC film test 2, c) NaCMC2 film, d) NaCMC3 film, e) NaCMC3 film without citric acid cross-linker.

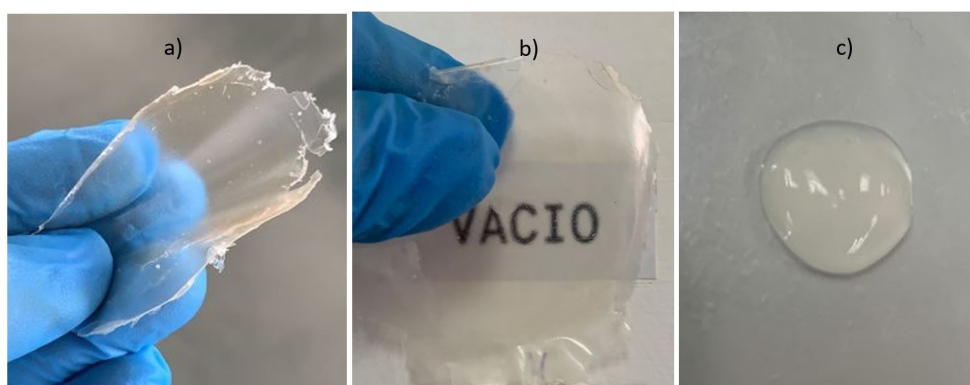


FIGURE 4.22: Hydrogel formed with NaCMC3 and 20% phenolic extract in solution. a) Proof of flexibility of dry hydrogel film. b) Proof of transparency of dry hydrogel film. c) Proof of gelation before drying.



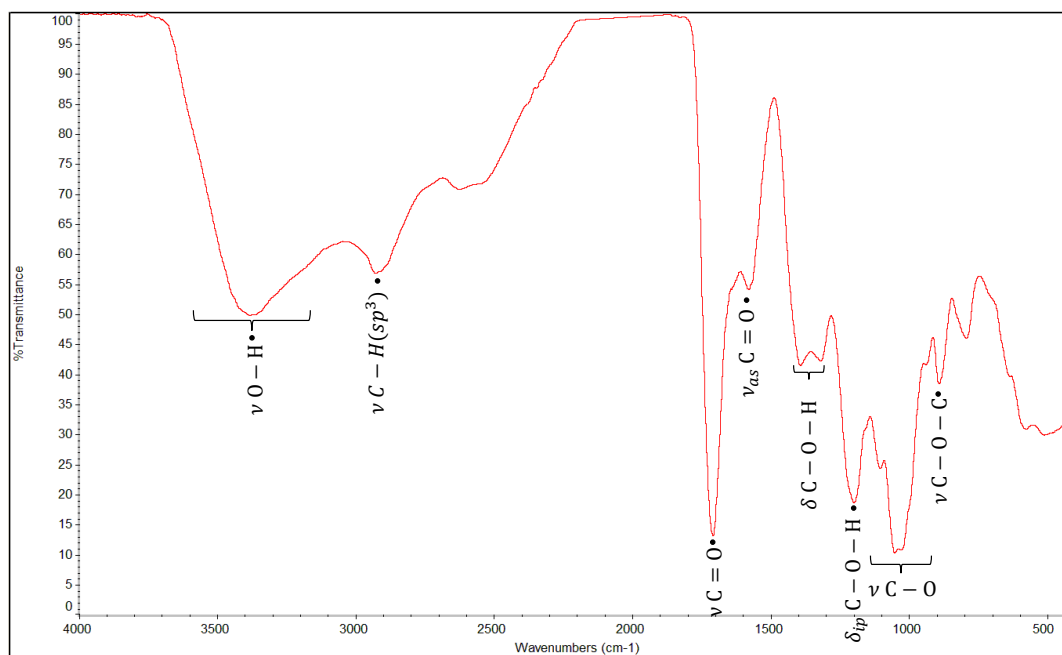


FIGURE 4.23: NaCMC3 film FTIR spectra .

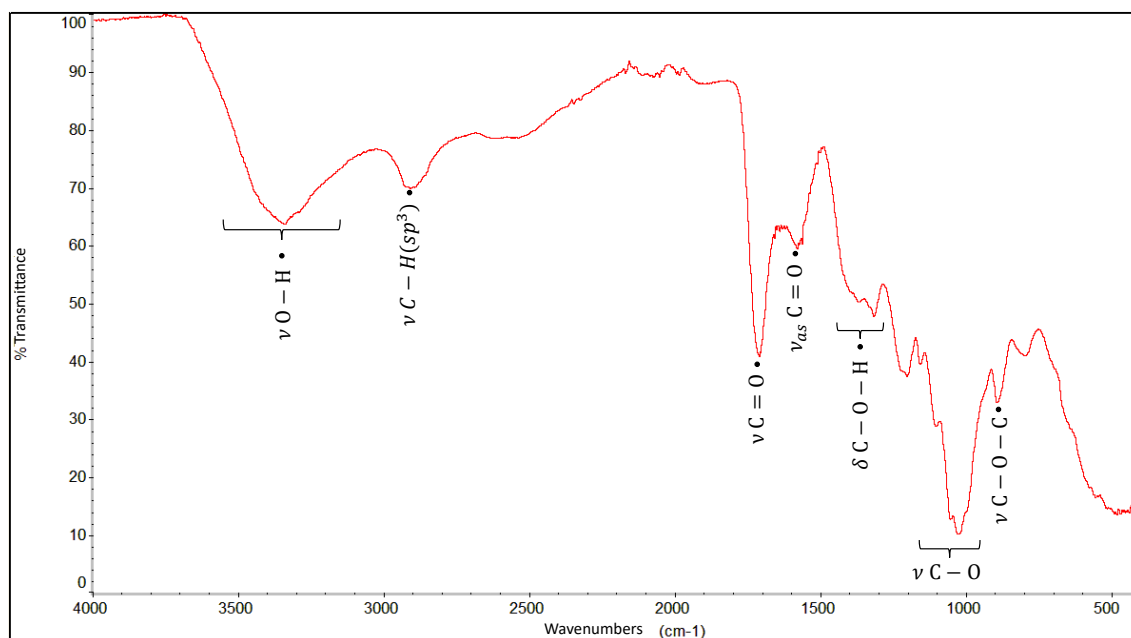


FIGURE 4.24: NaCMC2 film FTIR spectra.

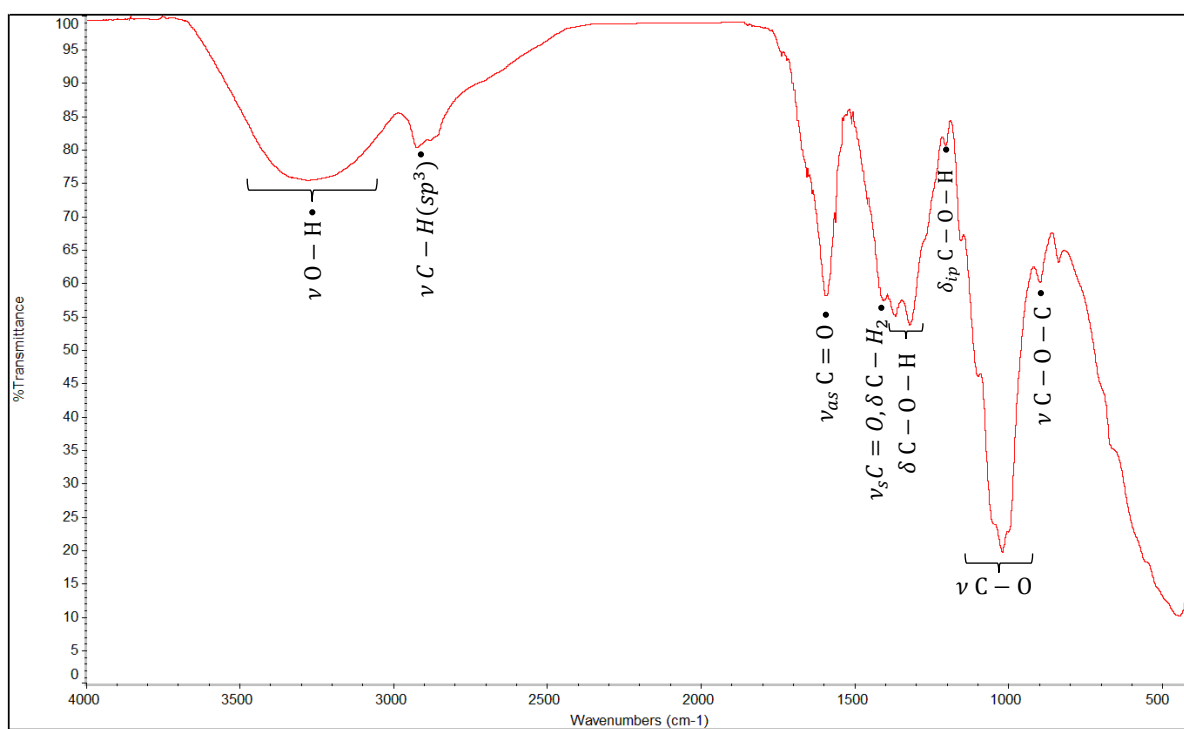


FIGURE 4.25: NaCMC3 film without citric acid crosslinker FTIR spectra.



## Chapter 5

# Conclusions

- The extraction of high purity cellulose was possible by an alkali treatment followed by a bleaching treatment, the purity of the obtained cellulose was proved by the clean white appearance of the product and FTIR analysis of the cellulose, which show only cellulose characteristic bands, proving the absence of lignins and hemicellulose. The high crystallinity of the obtained cellulose was proven by X-ray diffraction.
- Carboxymethylation can be achieved from different values of monochloroacetic acid, sodium hydroxide, temperature, and reaction time, this is proved by the presence of characteristic carboxymethylcellulose FTIR bands in all the different synthetic products.
- The major difference between the different synthetic products is the number of subproducts and the solubility of the obtained carboxymethylcellulose that is related to the obtained degree of substitution, the quality of the product is directly related to the control of all the reaction variables, highlighting the control of excess of NaOH in solution and the temperature control under 70 °C.
- The presence of phenolic and polyphenolic components was prove by the positive results obtained from the phytochemical test, also a high quantity of phenolics is determined by the use of Folin–Ciocalteu assay.
- It is possible to form hydrogel films with high UV protection profile by the incorporation of phenolic extract to the purified carboxymethylcellulose, this is proved by the UV profiling of the films obtained, by a solid UV-VIS spectrophotometer.
- The flexibility of the obtained hydrogel films is related to the use of citric acid as a crosslinker but is also possible to obtain less flexible hydrogel films without the addition of citric acid crosslinker, by the phenolics activities as physical crosslinkers.

- It is recommendable to use a filter with medium particle size for the washing steps at cellulose extraction because the CPH cellulose is very viscous and makes it difficult to filtrate any liquid across it.
- It is recommendable to perform many items of washing during the purification procedure to make sure the elimination of any remained subproducts.
- Since the formed hydrogel films are very thin its recommendable to design a frame that allows performing UV profiling in a more precise and easy way.

## Chapter 6

# Recommendations and Future projections

### 6.1 Recommendations

- It is recommendable to use a filter with medium particle size for the washing steps at cellulose extraction because the CPH cellulose is very viscous and makes it difficult to filtrate any liquid across it.
- It is recommendable to perform many items of washing during the purification procedure to make sure the elimination of any remained subproducts.
- Since the formed hydrogel films are very thin its recommendable to design a frame that allows performing UV profiling in a more precise and easy way.

### 6.2 Future projections

- Is desired a comparison between different extraction methods for active ingredients to examine which method is more suitable and give the greater concentration of the target components.
- The present product was made with a combination of two varieties of cocoa fruit without discrimination of proportions; because of this, in order to categorize the quality and yield of the starting product, a differential analysis between different varieties is suggested.
- To commercialize the cosmeceutical product is necessary to review the regulations that apply for this kind of product and mainly work in the required biological test to discard any side effect onto the skin.

- It could be beneficial to study different ingredient combinations for gel formation in order to evaluate which gives better characteristics for the conservation and application of the final product.
- Examine the use of alternative methods for the delignification process, like for example enzymatic methods, to reduce the difficulties during this experimental part.

## **Appendix A**

### **Errors determination**

**A.1 Random errors in the y-direction**

**A.2 Estimated standard error of the determined phenolic concentration**



TABLE A.1: F-C data analysis

$y_i$	$x_i$	$(y_i - \hat{y}_i)$	$(y_i - \hat{y}_i)^2$	$(x_i - \bar{x})^2$
0.0058	0.00	0.0034	$1.16 \times 10^{-5}$	0.01501
0.1230	0.02	-0.0070	$4.93 \times 10^{-5}$	0.01051
0.2550	0.04	-0.0027	$7.02 \times 10^{-6}$	0.00681
0.5130	0.08	0.0001	$1.06 \times 10^{-8}$	0.00181
0.6490	0.10	0.0085	$7.19 \times 10^{-5}$	0.00051
0.7740	0.12	0.0059	$3.42 \times 10^{-5}$	0.00001
0.8960	0.14	0.0002	$5.14 \times 10^{-8}$	0.00031
1.0150	0.16	-0.0084	$7.06 \times 10^{-5}$	0.00141
$\sum_i$			0.000245	0.03635

TABLE A.2:  $Average_{S_{x_0}}$ 

$y_0$	$Diluted S_{x_0}$	$S_{x_0}$	$S_{x_0}^2$
0.413	0.00106145	0.0106145	0.0001126
0.227	0.00106147	0.0212229	0.0004506
0.106	0.00106150	0.0424598	0.0023661
		$Average_{S_{x_0}}$	0.0343961

# Bibliography

- (1) Gandini, A.; Naceur, M. In *Biopolymers – New Materials for Sustainable Films and Coatings*, Plackett, D., Ed., First Edit; John Wiley & Sons: 2011; Chapter 8, pp 151–178.
- (2) Mondragon, G.; Fernandes, S.; Retegi, A.; Peña, C.; Algar, I.; Eceiza, A.; Arbelaz, A. *Industrial Crops and Products* **2014**, *55*, 140–148.
- (3) Yu, L.; Dean, K.; Li, L. *Progress in Polymer Science (Oxford)* **2006**, *31*, 576–602.
- (4) Zugenmaier, P., *Springer Series in Wood Science Series Editors Professor Dr . Rupert Wimmer Department of Material Sciences and Process Engineering Springer Series in Wood Science*, 2008, p 12.
- (5) César, N. R.; Pereira-da Silva, M. A.; Botaro, V. R.; de Menezes, A. J. *Cellulose* **2015**, *22*, 449–460.
- (6) Jimat, D. N.; Putra, S. S. S.; Jamal, P.; Nawawi, W. M. F. W. In *Advances in Nanotechnology and Its Applications*, 2020.
- (7) Abe, K.; Yano, H. *Carbohydrate Polymers* **2011**, *85*, 733–737.
- (8) Souza, L. O.; Lessa, O. A.; Dias, M. C.; Tonoli, G. H. D.; Rezende, D. V. B.; Martins, M. A.; Neves, I. C. O.; de Resende, J. V.; Carvalho, E. E. N.; de Barros Vilas Boas, E. V.; de Oliveira, J. R.; Franco, M. *Carbohydrate Polymers* **2019**, *214*, 152–158.
- (9) Pillaiyar, T.; Manickam, M.; Namasivayam, V. *Journal of Enzyme Inhibition and Medicinal Chemistry* **2017**, *32*, 403–425.
- (10) Tsuji, N.; Moriwaki, S.; Suzuki, Y.; Takema, Y.; Imokawa, G. *Photochemistry and Photobiology* **2001**, *74*, 283.
- (11) Fahmy, Y.; Mansour, O. *Cellulose and Paper Dept., National Research Centre* **1966**, *XX*, 1–7.
- (12) Abdul Karim, A.; Azlan, A.; Ismail, A.; Hashim, P.; Abd Gani, S. S.; Zainudin, B. H.; Abdullah, N. A. *Journal of Cosmetic Dermatology* **2016**, *15*, 283–295.
- (13) Levin, J.; del Rosso, J. Q.; Momin, S. B. How much do we really know about our favorite cosmeceutical ingredients?, 2010.

- (14) Vaishali, K.; Ashwini, C.; Kshitija, D.; Digambar, N. *International Journal of Research in Pharmacy and Chemistry* **2013**, *3*, 308–316.
- (15) Tsai, T. C.; Hantash, B. M. *Clinical Medicine Insights: Dermatology* **2008**, 1–20.
- (16) Núñez-González, S.; Bedoya, E.; Simancas-Racines, D.; Gault, C. *SAGE Open Medicine* **2020**, *8*, 205031212091828.
- (17) Fors, M.; González, P.; Viada, C.; Falcón, K.; Palacios, S. *BMC Dermatology* **2020**, *20*, 4–9.
- (18) Jimat, D. N.; Syed Putra, S. S.; Jamal, P.; Fazli Wan Nawawi, W. M., *Advances in Nanotechnology and Its Applications*; Jameel, A. T., Yaser, A. Z., Eds.; Springer Nature Singapore: 2020, pp 97–105.
- (19) Pelegrini, B. L.; Ré, F.; de Oliveira, M. M.; Fernandes, T.; de Oliveira, J. H.; Oliveira Junior, A. G.; Girotto, E. M.; Nakamura, C. V.; Sampaio, A. R.; Valim, A.; de Souza Lima, M. M. *Macromolecular Materials and Engineering* **2019**, *304*, 1–32.
- (20) Daud, Z.; Sari, A.; Kassim, M.; Aripin, A. M.; Awang, H.; Hatta, Z. M.; Education, V.; Tun, U.; Onn, H.; Pahat, B. *Australian Journal of Basic and Applied Sciences* **2013**, *7*, 406–411.
- (21) Jimat, D. N.; Putra, F. A.; Sulaiman, S.; Nor, Y. A.; Mohamed Azmin, N. F.; Syed Putra, S. S. *Journal of Advanced Research in Fluid Mechanics and Thermal Sciences* **2019**, *55*, 199–208.
- (22) Liu, W.; Mohanty, A. K.; Drzal, L. T.; Askel, P.; Misra, M. *Journal of Materials Science* **2004**, *39*, 1051–1054.
- (23) Vriesmann, L. C.; de Mello Castanho Amboni, R. D.; De Oliveira Petkowicz, C. L. *Industrial Crops and Products* **2011**, *34*, 1173–1181.
- (24) Sartini; Djide, M. N.; Alam, G. *Journal of Tradisional Medicine* **2009**.
- (25) Helal, N. A.; Eassa, H. A.; Amer, A. M.; Eltokhy, M. A.; Edafiohgo, I.; Nounou, M. I., *Nutraceuticals' Novel Formulations: The Good, the Bad, the Unknown and Patents Involved*; **2**, 2019; Vol. 13, pp 105–156.
- (26) Wang, W.; Lu, K. J.; Yu, C. H.; Huang, Q. L.; Du, Y. Z. *Journal of Nanobiotechnology* **2019**, *17*, 1–15.
- (27) Epstein, H. *Clinics in Dermatology* **2009**, *27*, 453–460.
- (28) Abdul Karim, A.; Azlan, A.; Ismail, A.; Hashim, P.; Abd Gani, S. S.; Zainudin, B. H.; Abdullah, N. A. *BMC Complementary and Alternative Medicine* **2014**, *14*, 1–13.

- (29) Gromovaya, V. F.; Shapoval, G. S.; Mironyuk, I. E. *Russian Journal of General Chemistry* **2002**, *72*, 774–777.
- (30) Ratz-Yko, A.; Arct, J.; Majewski, S.; Pytkowska, K. *Phytotherapy Research* **2015**, *29*, 509–517.
- (31) Zillich, O. V.; Schweiggert-Weisz, U.; Eisner, P.; Kersch, M. *International Journal of Cosmetic Science* **2015**, *37*, 455–464.
- (32) Nichols, J. A.; Katiyar, S. K. *Archives of Dermatological Research* **2010**, *302*, 71–83.
- (33) Pietta, P. G. *Journal of Natural Products* **2000**, *63*, 1035–1042.
- (34) Ronsisvalle, S.; Panarello, F.; Longhitano, G.; Siciliano, E. A.; Montenegro, L.; Panico, A. *Cosmetics* **2020**, *7*, 1–14.
- (35) Bae, J.; Kim, N.; Shin, Y.; Kim, S.-Y.; Kim, Y.-J. *Biomedical Dermatology* **2020**, *4*, 1–10.
- (36) Scott, B. C.; Butler, J.; Halliwell, B.; Aruoma, O. I. *Free Radical Research* **1993**, *19*, 241–253.
- (37) Graßmann, J. *Vitamins and Hormones* **2005**, *72*, 505–535.
- (38) Farris, P.; Krutmann, J.; Li, Y. H.; McDaniel, D.; Krol, Y. *Journal of Drugs in Dermatology* **2013**, *12*, 1389–1394.
- (39) Baxter, R. A. *Journal of Cosmetic Dermatology* **2008**, *7*, 2–7.
- (40) Imokawa, G.; Ishida, K. *International Journal of Molecular Sciences* **2015**, *16*, 7753–7775.
- (41) Ando, H.; Wen, Z. M.; Kim, H. Y.; Valencia, J. C.; Costin, G. E.; Watabe, H.; Yasumoto, K. I.; Niki, Y.; Kondoh, H.; Ichihashi, M.; Hearing, V. J. *Biochemical Journal* **2006**, *394*, 43–50.
- (42) Ando, H.; Watabe, H.; Valencia, J. C.; Yasumoto, K. I.; Furumura, M.; Funasaka, Y.; Oka, M.; Ichihashi, M.; Hearing, V. J. *Journal of Biological Chemistry* **2004**, *279*, 15427–15433.
- (43) Shigeta, Y.; Imanaka, H.; Ando, H.; Ryu, A.; Oku, N.; Baba, N.; Makino, T. *Biological and Pharmaceutical Bulletin* **2004**, *27*, 591–594.
- (44) Saewan, N.; Jimtaisong, A. *Journal of Applied Pharmaceutical Science* **2013**, *3*, 129–141.
- (45) Solano, F. *Molecules* **2020**, *25*, 1–18.

- (46) Sánchez-Rabaneda, F.; Jáuregui, O.; Casals, I.; Andrés-Lacueva, C.; Izquierdo-Pulido, M.; Lamuela-Raventós, R. M. Liquid chromatographic/electrospray ionization tandem mass spectrometric study of the phenolic composition of cocoa (*Theobroma cacao*), 2003.
- (47) Abeysinghe, D. C.; Kumari, I. P. N. P. *Journal of Food and Agriculture* **2012**, *5*, 5.
- (48) Rehman, A.; Jafari, S. M.; Tong, Q.; Riaz, T.; Assadpour, E.; Aadil, R. M.; Niaz, S.; Khan, I. M.; Shehzad, Q.; Ali, A.; Khan, S. *Advances in Colloid and Interface Science* **2020**, *284*, DOI: 10.1016/j.cis.2020.102251.
- (49) Zhang, Z.; Tsai, P. C.; Ramezanli, T.; Michniak-Kohn, B. B. *Wiley Interdisciplinary Reviews: Nanomedicine and Nanobiotechnology* **2013**, *5*, 205–218.
- (50) Global Cancer Observatory Ecuador: Incidence, Mortality and Prevalence by cancer site, <https://gco.iarc.fr/today/data/factsheets/populations/218-ecuador-fact-sheets.pdf>, Accessed: 2021-10-09, 2020.
- (51) Fors, M.; Palacios, S.; Falcon, K.; Ventimilla, K.; Simbaña, L.; Lagos, C.; Lasso, N.; Navas, C. *BMC Dermatology* **2018**, *18*, 1–5.
- (52) Arjona, R. H.; Piñeiros, J.; Ayabaca, M.; Freire, F. H. *Annali dell'Istituto Superiore di Sanita* **2016**, DOI: 10.4415/ANN\_16\_03\_08.
- (53) Saraf, S.; Kaur, C. *Pharmacognosy Reviews* **2010**, *4*, 1–11.
- (54) Milam, E. C.; Rieder, E. A. *Journal of Drugs in Dermatology* **2016**, DOI: 10.1002/9781119680116.ch4.
- (55) Davis, S. C.; Perez, R. *Clinics in Dermatology* **2009**, *27*, 502–506.
- (56) Kligman, D. *DERMATOLOGIC CLINICS* **2000**, *18*, 609–615.
- (57) Amer, M.; Maged, M. *Clinics in Dermatology* **2009**, *27*, 428–430.
- (58) Choi, C. M.; Berson, D. S. *Seminars in Cutaneous Medicine and Surgery* **2006**, *25*, 163–168.
- (59) Lage, R.; Mendes, C.; Abdalla, B. M. Z.; Arbiser, J.; Costa, A. In *Daily Routine in Cosmetic Dermatology*, 2016.
- (60) Monteiro, E. d. O.; Baumann, L. S. *Expert Review of Dermatology* **2006**, *1*, 379–389.
- (61) Dreher, F.; Maibach, H. *Current problems in dermatology* **2001**, *29*, 157–164.
- (62) Burke, K. E. *Mechanisms of Ageing and Development* **2018**, *172*, 123–130.
- (63) Addor, F. A. S. *Anais Brasileiros de Dermatologia* **2017**, *92*, 356–362.

- (64) Rudolf, J.; Raad, H.; Taieb, A.; Rezvani, H. R. *Antioxidants and Redox Signaling* **2018**, *28*, 1238–1261.
- (65) Pinnell, S. R. *Journal of the American Academy of Dermatology* **2003**, *48*, 1–22.
- (66) Chen, L.; Hu, J. Y.; Wang, S. Q. *Journal of the American Academy of Dermatology* **2012**, *67*, 1013–1024.
- (67) Burke, K. E. **2010**, 206–217.
- (68) Pecorelli, A.; McDaniel, D. H.; Wortzman, M.; Nelson, D. B. *Archives of Dermatological Research* **2021**, *313*, 139–146.
- (69) Martins, T. E. A.; Pinto, C. A. S. d. O.; de Oliveira, A. C.; Velasco, M. V. R.; Guitierrez, A. R. G.; Rafael, M. F. C.; Tarazona, J. P. H.; Retuerto-Figueroa, M. G. *Scientia Pharmaceutica* **2020**, *88*, 1–17.
- (70) Kaur, I. P.; Kapila, M.; Agrawal, R. *Ageing Research Reviews* **2007**, *6*, 271–288.
- (71) Polaskova, J.; Pavlackova, J.; Egner, P. *Skin Research and Technology* **2015**, *21*, 403–412.
- (72) Hougeir, F. G.; Kircik, L. *Dermatologic Therapy* **2012**, *25*, 234–237.
- (73) Rahman, H. S.; Othman, H. H.; Hammadi, N. I.; Yeap, S. K.; Amin, K. M.; Samad, N. A.; Alitheen, N. B. *International Journal of Nanomedicine* **2020**, *15*, 2439–2483.
- (74) Dutta, S. D.; Patel, D. K.; Lim, K. T. *Journal of Biological Engineering* **2019**, *13*, 1–19.
- (75) Catoira, M. C.; Fusaro, L.; Di Francesco, D.; Ramella, M.; Boccafoschi, F. *Journal of Materials Science: Materials in Medicine* **2019**, *30*, DOI: 10.1007/s10856-019-6318-7.
- (76) De Amorim, J. D. P.; de Souza, K. C.; Duarte, C. R.; da Silva Duarte, I.; de Assis Sales Ribeiro, F.; Silva, G. S.; de Farias, P. M. A.; Stingl, A.; Costa, A. F. S.; Vinhas, G. M.; Sarubbo, L. A. *Environmental Chemistry Letters* **2020**, *18*, 851–869.
- (77) Costa, R.; Santos, L. *Powder Technology* **2017**, *322*, 402–416.
- (78) Jones, D.; Ormondroyd, G. O.; Curling, S. F.; Popescu, C. M.; Popescu, M. C., *Chemical compositions of natural fibres*, 2017, pp 23–58.
- (79) Melikoğlu, A. Y.; Bilek, S. E.; Cesur, S. *Carbohydrate Polymers* **2019**, *215*, 330–337.
- (80) Chen, H.; Wang, L. *Technologies for Biochemical Conversion of Biomass* **2017**, 21–64.

- (81) Ouarhim, W.; Zari, N.; Bouhfid, R.; Qaiss, A. E. K. *Mechanical and Physical Testing of Biocomposites, Fibre-Reinforced Composites and Hybrid Composites* **2018**, 43–60.
- (82) Ginting, M.; Utama, A.; Muhammad, H.; Maulida; Tambun, R *IOP Conference Series: Materials Science and Engineering* **2021**, 1122, 012094.
- (83) Yáñez-S, M.; Matsuhira, B.; Maldonado, S.; González, R.; Luengo, J.; Uyarte, O.; Serafine, D.; Moya, S.; Romero, J.; Torres, R.; Kogan, M. J. *Cellulose* **2018**, 25, 2901–2914.
- (84) Manousi, N.; Sarakatsianos, I.; Samanidou, V., *Extraction Techniques of Phenolic Compounds and Other Bioactive Compounds From Medicinal and Aromatic Plants*; Elsevier Inc.: 2019, pp 283–314.
- (85) International Centre for Science and Technology, *Extraction Technologies for Medicinal and Aromatic Plant*, Earth, Env; Sukhdev Swami Handa, Suman Preet Singh Khanuja, Gennaro Longo Dutt, R. D., Ed.; International Centre for Science and High Technology: Trieste, Italy, 2008; Vol. 148, pp 148–162.
- (86) Predescu, N. C.; Papuc, C.; Nicorescu, V.; Gajaila, I.; Goran, G. V.; Petcu, C. D.; Stefan, G. *Revista de Chimie* **2016**, 67, 1922–1927.
- (87) Gebregergs, A. *Addis Ababa University Addis* **2021**.
- (88) Annuar, A. S.; Rahman, R. A.; Munir, A.; Murad, A.; El-enshasy, H. A.; Illias, R. *Carbohydrate Polymers* **2021**, 118159.
- (89) Mali, K. K.; Dhawale, S. C.; Dias, R. J.; Dhane, N. S.; Ghorpade, V. S. *Indian Journal of Pharmaceutical Sciences* **2018**, 80, 657–667.
- (90) Sannino, A.; Demitri, C.; Madaghiele, M. *Materials* **2009**, 2, 353–373.
- (91) Johar, N.; Ahmad, I.; Dufresne, A. *Industrial Crops and Products journal* **2012**, 37, 93–99.
- (92) Iyabode, A.; Felicia, L.; Okunola, A.; Ajao, J.; Victor, T. *Heliyon Research* **2021**, 7, DOI: <https://doi.org/10.1016/j.heliyon.2021.e06680>.
- (93) Park, S.; Baker, J. O.; Himmel, M. E.; Parilla, P. A.; Johnson, D. K. *Biotechnology for Biofuels* **2010**, 3, 1–10.
- (94) Shui, T.; Feng, S.; Chen, G.; Li, A.; Yuan, Z.; Shui, H.; Kuboki, T.; Xu, C. *Biomass and Bioenergy* **2017**, 105, 51–58.
- (95) Rachtanapun, P.; Klunklin, W.; Jantrawut, P.; Leksawasdi, N.; Jantanasakulwong, K.; Phimolsiripol, Y.; Seesuriyachan, P.; Chaiyaso, T.; Ruksiriwanich, W.; Phongthai, S.; Sommano, S. R.; Punyodom, W.; Reungsang, A.; Ngo, T. M. P. *Polymers* **2021**, 13, 1–13.

- (96) Chen, J.; Li, H.; Fang, C.; Cheng, Y.; Tan, T.; Han, H. *Carbohydrate Polymers journal* **2020**, 237, DOI: <https://doi.org/10.1016/j.carbpol.2020.116040>.
- (97) Yuldoshov, S.; GoyipovI, S.; Sarymsakov, A *International Journal of Advanced Science and Technology* **2020**, 29, 4733–4737.
- (98) Sharma, V.; Agarwal, A.; Chaudhary, U.; Singh, M. *International Journal of Pharmacy and Pharmaceutical Sciences* **2013**, 5, 3–6.
- (99) Sonam, M.; Singh, R. P.; Pooja, S. *International Journal of Pharmacognosy and Phytochemical Research* 2017; **2017**, 9(4), 523–527 DOI.
- (100) Saptarini, N. Y. I. M.; Herawati, I. E.; Permatasari, U. L. I. Y. *Asian Journal of Pharmaceutical and Clinical Research* **2016**, 9, 10–12.
- (101) Mamta, S.; Jyoti, S. *International research journal of pharmacy* **2012**, 3, 324–326.
- (102) Ali, S.; Khan, M. R.; Sajid, M.; Zahra, Z. *BMC Complementary and Alternative Medicine* **2018**, 1–15.
- (103) Gul, R.; Jan, S. U.; Faridullah, S.; Sherani, S.; Jahan, N. *The Scientific World Journal* **2017**, 2017, 7.
- (104) Dinakaran, S. K.; Chelle, S.; Avasarala, H. *Journal of Traditional and Complementary Medicine* **2019**, 9, 319–327.
- (105) Ainsworth, E. A.; Gillespie, K. M. *Nature Protocols* **2007**, 2, 875–877.
- (106) Zhang, H.; Fu, S.; Chen, Y. *International Journal of Biological Macromolecules* **2020**, 147, 607–615.
- (107) Hubbell, C. A.; Ragauskas, A. J. *Bioresource Technology* **2010**, 101, 7410–7415.
- (108) Jeanes, A.; Isbell, H. *Journal of Research of the National Bureau of Standards* **1941**, 27, 125.
- (109) Yogendra, P. Diana, W., Lisa, I., Patricia, M., Mark, O. *Epa* **2000**, 56, 1–49.
- (110) Nindiyasari, F.; Griesshaber, E.; Zimmermann, T.; Manian, A. P.; Randow, C.; Zehbe, R.; Fernandez-Diaz, L.; Ziegler, A.; Fleck, C.; Schmahl, W. W. *Journal of Composite Materials* **2016**, 50, 657–672.
- (111) Wang, T.; Zhao, Y. *Carbohydrate Polymers journal* **2021**, 253, DOI: <https://doi.org/10.1016/j.carbpol.2020.117225>.
- (112) Lakshmi, D. S.; Trivedi, N.; Reddy, C. R. K. *Carbohydrate Polymers journal* **2016**, 157, 1604–1610.
- (113) Haleem, N.; Arshad, M.; Shahid, M.; Ashraf, M. *Carbohydrate Polymers* **2014**, 113, 249–255.



- (114) Horikawa, Y.; Hirano, S.; Mihashi, A.; Kobayashi, Y. *Applied Biochemistry and Biotechnology* **2019**, *188*, 1066–1076.
- (115) Rachtanapun, P. *Kasetsart Journal - Natural Science* **2009**, *43*, 259–266.
- (116) Ramli, S.; Mohamad, S.; Asri, M.; Sisak, A. *Malaysian Journal of Analytical Sciences* **2015**, *19*, 275–283.
- (117) Librando, V.; Lorusso, S. *CONSERVATION SCIENCE IN CULTURAL HERITAGE* **2011**, 249–268.
- (118) Pavia, D. L.; Lampman, G. M.; Kriz, G. S.; Vyvyan, J. R., *INTRODUCTION TO SPECTROSCOPY*; Cengage Learning: Washington, 2015, pp 14–30.
- (119) Mahdi, S. *Maderas. Ciencia y tecnología* **2019**, *21*, 381–392.
- (120) Zong, Y.; Zhang, Y. *RSC Advances* **2017**, *7*, 31352–31364.
- (121) Riaz, T.; Zeeshan, R.; Zarif, F.; Ilyas, K.; Muhammad, N.; Safi, S. Z.; Rahim, A.; Rizvi, S. A. A.; Rehman, I. U. *Applied Spectroscopy Reviews* **2018**, *53*, 703–746.
- (122) Asl, S. A.; Mousavi, M.; Labbafi, M. *Journal of Food Processing & Technology* **2017**, *8*, DOI: 10.4172/2157-7110.1000687.
- (123) Dieckman, S. F.; Jarrell, J. G.; Voris, R. S. *Industrial & Engineering Chemistry* **1953**, *45*, 2287–2290.
- (124) Miller, J.; Miller, J.; Miller, R., *Statistics and Chemometrics for Analytical Chemistry*, Seventh Ed; Weston, P., Ed.; 4; Pearson Education Limited: Harlow, United Kingdom, 2004; Vol. 46, pp 498–499.
- (125) Wu, J. I. N.; Chiu, S.-c.; Pearce, E. L. I. M.; Kwei, T. K. *Journal of Polymer Science* **2000**, *39*, 224–231.